Evaluation of the updated YSU planetary boundary layer scheme within WRF for wind resource and air quality assessments

Xiao-Ming Hu,[1] Petra M. Klein,[1,2] and Ming Xue[1,2]

Received 12 March 2013; revised 5 September 2013; accepted 8 September 2013; published 24 September 2013.

[1] In previous studies, the Yonsei University (YSU) planetary boundary layer (PBL) scheme implemented in the Weather Research and Forecasting (WRF) model was reported to perform less well at night, while performing better during the day. Compared to observations, predicted nocturnal low-level jets (LLJs) were typically weaker and higher. Also, the WRF model with Chemistry (WRF/Chem) with the YSU scheme was reported to sometimes overestimate near-surface ozone (O_3) concentration during the nighttime. The updates incorporated in WRF version 3.4.1, include modifications of the nighttime velocity scale used in the YSU boundary layer scheme. The impacts of this update on the prediction of nighttime boundary layers and related implications for wind resource assessment and air quality simulations are examined in this study. The WRF/Chem model with the updated YSU scheme predicts smaller eddy diffusivities in the nighttime boundary layer, and consequently lower and stronger LLJs over a domain focusing on the southern Great Plains area, showing a better agreement with the observations. As a result, related overestimation problems for near-surface temperature and wind speeds appear to be resolved, and the nighttime minimum near-surface O_3 concentrations are better captured. Simulated vertical distributions of meteorological and chemical variables for weak wind regimes (e.g., in the absence of LLJ) are less impacted by the YSU updates.

Citation: Hu, X.-M., P. M. Klein, and M. Xue (2013), Evaluation of the updated YSU planetary boundary layer scheme within WRF for wind resource and air quality assessments, *J. Geophys. Res. Atmos.*, *118*, 10,490–10,505, doi:10.1002/jgrd.50823.

1. Introduction

[2] Accurate simulations and forecasts of boundary layer winds are important for the wind power industry [*Storm and Basu*, 2010; *Carvalho et al.*, 2012], agriculture sectors [*Prabha and Hoogenboom*, 2008; *Prabha et al.*, 2011], and air quality management [*Bao et al.*, 2008; *Cheng et al.*, 2012; *Gilliam et al.*, 2012]. Planetary boundary layer (PBL) parameterization schemes are of vital importance for accurate simulations of wind, turbulence, and air quality in the lower atmosphere and thus play an important role for a number of applications [*Steeneveld et al.*, 2008; *Storm et al.*, 2009; *Carvalho et al.*, 2012; *Hu et al.*, 2012; *García-Díez et al.*, 2013]. PBL parameterization schemes have been steadily improved over the past few decades. However, errors and uncertainties associated with PBL schemes still remain one of the primary sources of inaccuracies of model simulations [*Zhang and Zheng*, 2004; *Pleim*, 2007a, 2007b; *Teixeira et al.*, 2008; *Hu et al.*, 2010a, 2010b, 2012; *Nielsen-Gammon et al.*, 2010]. While much progress has been made in simulating daytime convective boundary layer (CBL), progress with the modeling of nighttime boundary layer has been slower [*Salmond and McKendry*, 2005; *Beare et al.*, 2006; *Brown et al.*, 2008; *Hong*, 2010] and systematic overestimations of near-surface winds during stable conditions have been noticed in the simulations with several meteorological models [e.g., *Zhang and Zheng*, 2004; *Miao et al.*, 2008; *Han et al.*, 2008; *Shimada et al.*, 2011; *Vautard et al.*, 2012; *Garcia-Menendez et al.*, 2013; *Zhang et al.*, 2013; *Wolff and Harrold*, 2013].

[3] A few recent studies examined the sensitivity of the Weather Research and Forecasting (WRF) [*Skamarock et al.*, 2008] model predictions to PBL schemes [*Jankov et al.*, 2005, 2007; *Li and Pu*, 2008; *Borge et al.*, 2008; *Hu et al.*, 2010a, 2012; *Gilliam and Pleim*, 2010; *Mohan and Bhati*, 2011; *Xie et al.*, 2012, 2013; *Floors et al.*, 2013; *Sterk et al.*, 2013; *Yang et al.*, 2013; *Coniglio et al.*, 2013; *Yver et al.*, 2013]. The performance of different PBL schemes varies depending on the meteorological conditions, e.g., nonlocal PBL schemes were reported to perform better than local PBL schemes in the daytime CBL. However, *Shin and Hong* [2011] discuss that excessive daytime mixing, simulated by some nonlocal PBL schemes, may also lead to overly mixed vertical profiles in the residual layer. In general, local PBL schemes appear to provide a more realistic representation of the nighttime boundary layer [*Hu et al.*, 2010a; *Shin and Hong*, 2011; *Svensson et al.*, 2011; *Kolling et al.*, 2012; *LeMone et al.*, 2013], but further improvement of PBL schemes, especially for nighttime boundary layer, is

[1]Center for Analysis and Prediction of Storms, University of Oklahoma, Norman, Oklahoma, USA.
[2]School of Meteorology, University of Oklahoma, Norman, Oklahoma, USA.

Corresponding author: X.-M. Hu, Center for Analysis and Prediction of Storms, University of Oklahoma, Norman, Oklahoma 73072, USA. (xhu@ou.edu)

2169-897X/13/10.1002/jgrd.50823

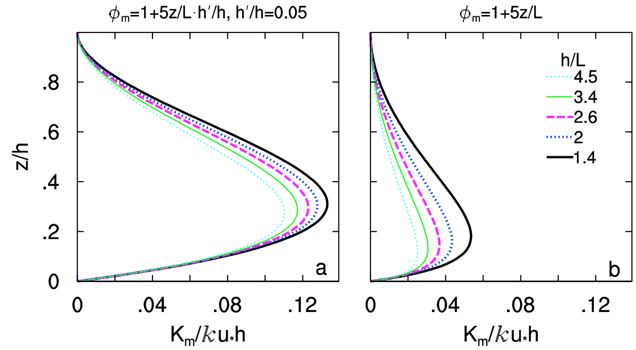

Figure 1. Vertical profiles of dimensionless momentum eddy diffusivity K_m under different stabilities (different h/L) computed by the YSU scheme implemented in (a) the earlier versions of WRF (i.e., 3.4 and earlier) and (b) WRF 3.4.1.

urgently warranted [*Hanna and Yang*, 2001; *Zilitinkevich et al.*, 2007; *Teixeira et al.*, 2008; *Grisogono and Belusic*, 2008; *Fernando and Weil*, 2010; *Grisogono*, 2010; *Lareau et al.*, 2013; *Sterk et al.*, 2013].

[4] Most evaluation and improvement work of air quality models focused on peak ozone (O_3) values during the daytime (i.e., the maximum 1 h or maximum 8 h running average O_3 mixing ratios). As a result, some models are overtuned to achieve acceptable model-to-data error statistics in terms of maximum 1 h or maximum 8 h average O_3, while they perform less well for periods with lower O_3 concentrations (e.g., nighttime, *Arnold and Dennis*, 2001; *Mebust et al.*, 2003; *Hu*, 2008; *Stockwell et al.*, 2013). Overestimation of nighttime surface O_3 is a common problem for many air quality models [*Mao et al.*, 2006; *Chen et al.*, 2006; *Chen et al.*, 2008; *Engardt*, 2008; *Zhang et al.*, 2009; *Lin and McElroy*, 2010; *Hu et al.*, 2010c; *Žabkar et al.*, 2011]. Such overestimation of nighttime surface O_3 is speculated to be partially due to incorrect model representation of the PBL [*Eder et al.*, 2006; *Herwehe et al.*, 2011; *Žabkar et al.*, 2011], underestimation of O_3 dry deposition [*Mao et al.*, 2006; *Chen et al.*, 2006; *Chen et al.*, 2008; *Zhang et al.*, 2009; *Lin and McElroy*, 2010], and/or uncertainties in emissions [*Žabkar et al.*, 2011]. In this study we will examine the impact of vertical mixing treatment on the prediction of nighttime boundary layer structure and O_3 concentration.

[5] The Yonsei University (YSU) [*Hong et al.*, 2006; *Hong*, 2010] PBL scheme is a first-order nonlocal scheme, with a countergradient term and an explicit entrainment term in the turbulence flux equation. It has been widely used in meteorological and atmospheric chemistry simulations. The WRF model with the YSU PBL scheme appears to realistically capture the vertical structure of meteorological and chemical variables during the daytime, while it has been shown to have larger biases during nighttime [*Storm et al.*, 2009; *Hu et al.*, 2012]. Simulations with WRF versions 2.1, 2.2, and 3.1.1 using the YSU scheme are found to severely underestimate the nighttime wind speed shear exponent [*Storm and Basu*, 2010]. Other studies [e.g., *Storm et al.*, 2009; *Shin and Hong*, 2011; *Deppe*, 2011; *Hu et al.*, 2012; *Schumacher et al.*, 2013; *Draxl et al.*, 2012; *Floors et al.*, 2013] also reported that WRF (versions 2.2, 3.1, 3.1.1, 3.2, 3.2.1, and 3.4) with the YSU scheme tends to destroy the boundary layer vertical wind gradient during nighttime. As it turned out, such large nighttime biases in all versions between 3.0 and 3.4 of the WRF model were at least partially due to excessively strong mixing during nighttime that can be attributed to a coding bug in the YSU scheme implemented in the early versions of WRF. This bug has been fixed in WRF version 3.4.1. One of the goals of this paper is to document the impact of this bug fix on the prediction of boundary layer meteorology and O_3 in three-dimensional simulations using the WRF/Chem model [*Grell et al.*, 2005].

[6] The rest of this paper is organized as follows: in section 2, recent modifications to the YSU scheme and design of simulation experiments are described. In section 3, results of numerical experiments including prediction of boundary layer wind, temperature, wind profile exponent, and O_3 are presented. The paper concludes in section 4 with a summary of the main findings and a discussion about the need for future research.

2. The YSU PBL Scheme and Simulation Experiments

2.1. Modifications to the YSU PBL Scheme in WRF

[7] In the YSU PBL scheme, the momentum eddy diffusivity for the stable boundary layer is formulated as

$$K_m = kw_s z\left(1 - \frac{z}{h}\right)^2, \tag{1}$$

where ($w_s = u_*/\phi_m$) is the velocity scale, k is the von Karman constant, z is the height above ground, and h is the boundary layer height diagnosed using a critical Richardson number (0.25 over the land, while it depends on the surface winds and Rossby number over oceans). In the WRF before version 3.4.1, the nondimensional profile function, ϕ_m, for stable conditions in YSU was implemented as

$$\phi_m = 1 + 5\frac{z}{L}\cdot\frac{h'}{h}, \tag{2}$$

where L is the Monin-Obukov length, h' is the boundary layer height diagnosed using a critical Richardson number of 0 (S. Hong, personal communication, 2012). Since version 3.4.1, the formulation has been changed to

$$\phi_m = 1 + 5\frac{z}{L}, \tag{3}$$

which should be the correct implementation. Given the different estimation of h' and h, the factor $\frac{h'}{h}$ is always smaller than 1 and could be as small as 0.05 in the presence of strong vertical wind shear (e.g., in the presence of a low-level jet). Thus, the values of ϕ_m in the revised YSU scheme implemented in WRF version 3.4.1 are always larger than the corresponding values given by earlier versions. Example profiles of dimensionless K_m using the two versions of ϕ_m are shown in Figure 1. The K_m values using the updated ϕ_m (Figure 1b) are significantly smaller than those given by the old formulation (Figure 1a); the peak values of the K_m profiles are generally reduced more than half, and are reduced even more for higher stability (i.e., larger values of ${}^{h}/_{L}$). The heights of the profile peaks are also lower; effectively bringing the strongest mixing closer to the ground. The updated profiles (Figure 1b) appear to better capture the vertical mixing characteristics in the stable boundary layer [*Brost*

Table 1. Summary of Five Numerical Experiments Conducted With WRF/Chem

Abbreviation	WRF Version	PBL Scheme	Surface Layer Scheme[a] (Option Number in WRF)
YSU3.4	3.4	old YSU	MM5 similarity (1)
YSU3.4+	3.4	updated YSU	MM5 similarity (1)
YSU3.4.1	3.4.1	updated YSU	MM5 similarity (1)
MYJ	3.4.1	MYJ	Eta similarity (2)
BouLac	3.4.1	BouLac	Eta similarity (2)

[a]In the WRF model, some PBL schemes are tied to particular surface layer schemes [*Skamarock et al*., 2008], so a single common surface layer scheme could not be used here.

and Wyngaard, 1978]. Starting with version 3.4.1, an artificial lower limit for the velocity scale, $w_s \geq \frac{u_*}{5}$, found in the earlier versions of the YSU scheme has also been removed in addition to the change given in 3. The eddy diffusivity for scalars is computed from K_m by dividing it by the Prandtl number Pr. It thus experiences a similar change as K_m.

[8] In this study, the impact of the modifications to the YSU scheme on the prediction of boundary layer meteorology and air quality in the Great Plains for a low-level jets (LLJs) episode in July 2003 is investigated in three-dimensional simulations using the WRF model including its Chemistry model component (WRF/Chem) [*Grell et al*., 2005]. The performance of the YSU scheme is also assessed against simulations with WRF/Chem 3.4.1 using the Mellor-Yamada-Janjić [*Janjic*, 1990] and Bougeault–Lacarrére [*Bougeault and Lacarrere*, 1989] PBL schemes. These two PBL schemes were selected for the comparison because they both diagnose turbulent diffusion coefficient for scalars, which is required for WRF/Chem simulations [*Hu et al*., 2012; *Pleim*, 2011] and because they were widely used/evaluated for both meteorology and air quality applications [e.g., *Shin and Hong*, 2011; *Xie et al*., 2012; *LeMone et al*., 2013; *Žabkar et al*., 2013]. MYJ and BouLac are both local TKE closure (one-and-a-half order closure) PBL schemes, but with different mixing length and model parameters. MYJ showed better performance during stable conditions than some nonlocal scheme [*Shin and Hong*, 2011; *Draxl et al*., 2012] while BouLac had a nighttime overmixing problem when the mixing length is computed with the standard set of parameters of the scheme [*Bravo et al*., 2008].

2.2. Three-Dimensional Simulations

[9] To investigate the impact of vertical mixing treatments in the YSU scheme on nighttime boundary layer meteorology and air quality, five simulations are conducted with different versions of WRF/Chem. The first two simulations are conducted with the officially released WRF/Chem versions 3.4 and 3.4.1 and the YSU PBL scheme (these simulations are in the following referred to as YSU3.4 and YSU3.4.1). In addition to the update to the YSU scheme, there are other updates in the WRF/Chem model from versions 3.4 to 3.4.1. To isolate the impact of the update to the YSU scheme, the YSU scheme from WRF/Chem 3.4.1 is implemented into WRF/Chem 3.4. This modified version of WRF/Chem is used for the third simulation (in the following referred to as YSU3.4+). Additionally, two WRF/Chem 3.4.1 simulations with MYJ and BouLac (in the following referred to as MYJ and BouLac) are conducted to compare with the three YSU simulations and observations. Table 1 summarizes all the five numerical experiments regarding their abbreviations and differences.

[10] For all five simulations, two one-way nested domains (Figure 2) are employed with horizontal grid spacings of 22.5 and 4.5 km, respectively. Each domain has 48 vertical layers extending from the surface to 100 hPa. The lowest 20 model

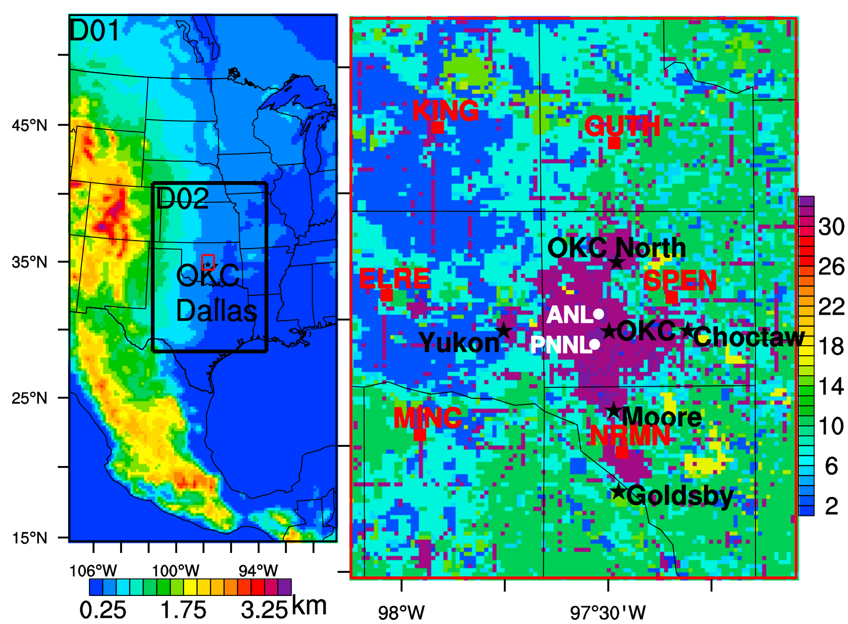

Figure 2. (left) Map of model domains and terrain height (background color) used in this study. (right) The zoomed in land use categories in the red box around Oklahoma City (OKC). The locations of the six EPA sites in the OKC metropolitan area (i.e., Choctaw, Goldsby, Moore, OKC, OKC North, and Yukon), six Mesonet sites around OKC (i.e., ELRE, GUTH, KING, MINC, NRMN, and SPEN), and the ANL (Argonne National Laboratory) and PNNL (Pacific Northwest National Laboratory) sites are marked.

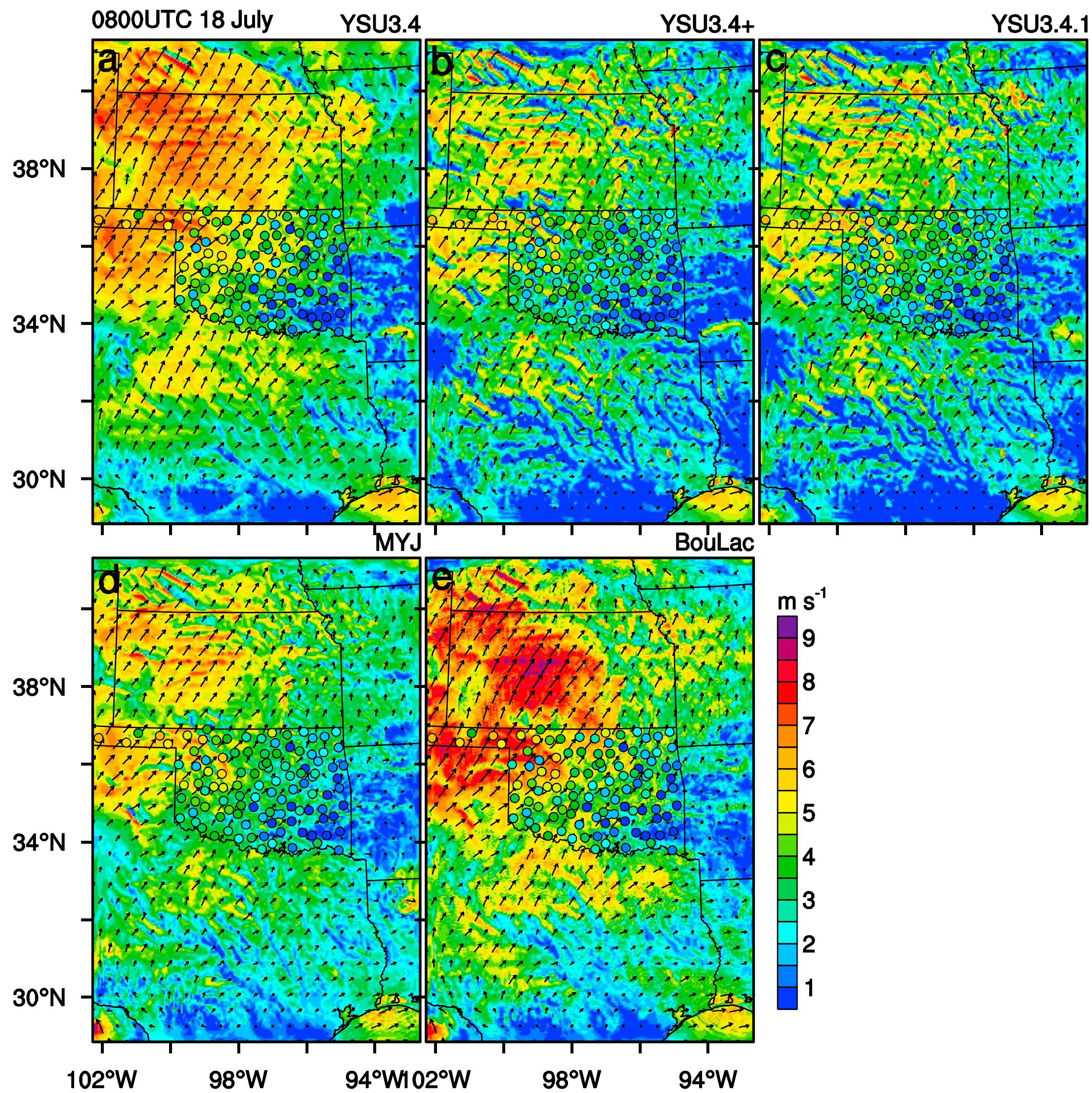

Figure 3. The 10 m wind speed at 0800 UTC on 18 July 2003 simulated by the numerical experiments (a) YSU3.4, (b) YSU3.4+, (c) YSU3.4.1, (d) MYJ, and (e) BouLac. The observed values are indicated by shaded circles.

sigma levels are at 1.0, 0.997, 0.994, 0.991, 0.988, 0.985, 0.975, 0.97, 0.96, 0.95, 0.94, 0.93, 0.92, 0.91, 0.895, 0.88, 0.865, 0.85, 0.825, and 0.8 (the corresponding midlevel heights of each model layer are about 12, 37, 61, 86, 111, 144, 186, 227, 290, 374, 459, 545, 631, 717, 826, 958, 1092, 1226, and 1409 m above ground). All model domains use the Dudhia shortwave radiation algorithm [*Dudhia*, 1989], the rapid radiative transfer model (RRTM) [*Mlawer et al*., 1997] for longwave radiation, the WRF Single-Moment 6-Class (WSM6) microphysics scheme [*Hong et al*., 2004], and the Noah Land-Surface Scheme [*Chen and Dudhia*, 2001]. For urban regions within domain 2 (shown in purple in Figure 2b), a single-layer urban canopy model (UCM) is used for land surface treatment. The 1° × 1° National Centers for Environmental Prediction (NCEP) Final (FNL) Global Forecast System (GFS) analyses are used for the initial and boundary conditions of all meteorological variables (including soil properties). The inner grid gets its boundary conditions from the outer grid forecast.

[11] To determine gas phase chemical reactions, the Regional Atmospheric Chemistry Mechanism (RACM), [*Stockwell et al*., 1997] implemented within WRF/Chem is used. Hourly anthropogenic emissions of chemical species come from the 4 km × 4 km national emission inventory (NEI) for year 2005. Biogenic emissions are calculated using established algorithms [*Guenther et al*., 1994]. The focus of our modeling study is an episode (17–19 July 2003) during the Joint Urban 2003 (JU2003) tracer experiment campaign in the Oklahoma City (OKC) metropolitan area [*Allwine et al*., 2004]. During this episode, the sky was clear, southerly/southwesterly wind dominated and moderate-strength LLJs occurred during the nighttime [*Lundquist and Mirocha*, 2008; *Hu et al*., 2013b]. Thus, the episode is ideal for testing the impact of the update to the YSU scheme for nighttime boundary layer, in particular for examining if the updated YSU scheme has better skill in simulating LLJs. The simulations are initialized at 0000 UTC 17 July and run until 0600 UTC 19 July 2003 without any data assimilation. The initial and boundary conditions for the

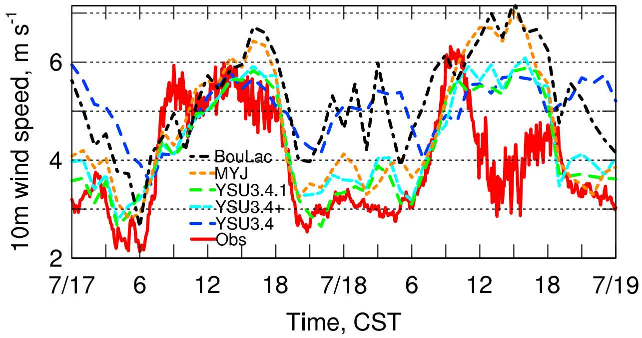

Figure 4. Observed and simulated average 10 m wind speed at the six Mesonet sites around OKC.

chemical species are extracted from the output of the global model MOZART4 with a resolution of 2.8° × 2.8° [*Emmons et al.*, 2010]. Similar model configurations were used in previous similar type of studies [e.g., *Hu et al.*, 2010c, 2012, 2013c; *Klein et al.*, 2013].

2.3. Data Sets for Model Evaluation

[12] During the JU2003 tracer experiment, multiple meteorological observation systems were deployed across the OKC metropolitan area. Boundary layer radar wind profilers and radiosonde are most relevant to the present study. The boundary layer wind profiler was operated almost continuously during the entire month of July 2003 in OKC at the Argonne National Laboratory (ANL) site [*De Wekker et al.*, 2004]. The wind profiler collected data with a vertical resolution of 55 m and an average interval of 25 min, providing coverage from 82 m to ~2700 m [*De Wekker et al.*, 2004]. Radiosonde profiles were taken at the Pacific Northwest National Laboratory (PNNL) site during four nighttime intensive observational periods (IOPs). The episode chosen for this study is one of the IOPs, and temperature profiles from the radiosonde releases during the night are included for our model evaluation. The PNNL and ANL sites were located approximately 2 km south and 5 km north of downtown OKC, respectively (Figure 2).

[13] Meteorological data collected by the Oklahoma Mesonet [*McPherson et al.*, 2007] and O_3 data collected at the Environmental Protection Agency (EPA) Air Quality System (AQS) sites (available at http://www.epa.gov/ttn/airs/airsaqs/detaildata/downloadaqsdata.htm) were additional data sources used to evaluate the modeling results in this study. With an average spacing of approximately 30 km between the Mesonet stations, there is at least one station in each Oklahoma county [*Fiebrich and Crawford*, 2001]. In contrast, the EPA AQS sites have a much more inhomogeneous distribution. They are clustered near urban areas and are relatively sparse in rural areas. The meteorological variables considered in this study included air temperature at 1.5 m above ground level (AGL) and wind speed at 10 m AGL.

3. Results of Numerical Experiments

3.1. Prediction of Boundary Layer Wind and Temperature

[14] Figure 3 shows the 10 m wind speeds at 0800 UTC (0200 LST), 18 July 2003 from the five simulations, as compared to Mesonet observations shown by colored circles. It is clear that the simulated nighttime near-surface winds are improved considerably with the updated YSU PBL scheme. In the YSU3.4 simulation, near-surface winds are significantly overestimated, especially for central and western Oklahoma where Mesonet data are available (Figure 3a); this problem is virtually eliminated in the YSU3.4.1 results (Figure 3c). The YSU3.4+ run, for which the updated YSU PBL scheme was implemented into WRF/Chem 3.4, shows similar results as the YSU3.4.1 simulation, indicating that the update to the YSU scheme plays a dominant role for the performance improvement from WRF versions 3.4 to 3.4.1. A more detailed investigation of the differences between the YSU3.4+ and YSU3.4.1 results is beyond the scope of the study. For the experiments with two other PBL schemes, MYJ simulates similar nighttime 10 m wind as YSU3.4+ and YSU 3.4.1, while BouLac simulates the highest 10 m wind speed, especially for the western Oklahoma (Figure 3e).

[15] Diurnal cycles of observed and simulated 10 m wind speeds averaged over the six Mesonet sites around OKC are compared in Figure 4. The impact of the update to the YSU scheme is most prominent during nighttime, while its impact on daytime prediction is negligible in terms of near-surface wind speeds. Detailed evaluation statistics based on nighttime, meteorological near-surface variables at the 111 Mesonet sites in Oklahoma are presented in Table 2. The WRF models capture the diurnal variation of surface wind speed well, with maximum/minimum wind speed during the daytime/nighttime (Figure 4). However, the WRF with the

Table 2. Statistics[a] for Nighttime 2 m Temperature and 10 m Wind Speed at All the Mesonet Sites[b] in Oklahoma for Five Simulations, i.e., YSU3.4, YSU3.4+, YSU3.4.1, MYJ, and BouLac

	2 m Temperature					10 m Wind Speed				
	YSU3.4	YSU3.4+	YSU3.4.1	MYJ	BouLac	YSU3.4	YSU3.4+	YSU3.4.1	MYJ	BouLac
Mean Obs	25.713	25.713	25.713	25.713	25.713	2.656	2.656	2.656	2.656	2.656
Mean Sim	27.94	25.761	25.732	25.172	26.441	4.181	2.99	2.943	3.362	3.99
Number of data	2436	2436	2436	2436	2436	2412	2412	2412	2412	2412
corr	0.86	0.871	0.869	0.862	0.85	0.643	0.579	0.582	0.662	0.597
MB	2.226	0.048	0.018	−0.541	0.727	1.525	0.334	0.287	0.706	1.334
MAGE	2.351	1.168	1.181	1.301	1.388	1.682	1.052	1.039	1.071	1.564
RMSE	2.732	1.51	1.519	1.619	1.745	1.951	1.343	1.325	1.325	1.912
NMB	0.087	0.002	0.001	−0.021	0.028	0.574	0.126	0.108	0.266	0.502

[a]The statistical metrics include: correlation coefficient (corr), mean bias (MB), mean absolute gross error (MAGE), root mean-square error (RMSE), normalized mean bias (NMB). Formulas for these metrics can be found in *Seigneur et al.* [2000]. These statistical metrics are commonly used in numerical model evaluations [e.g., *Yu et al.*, 2006; *Han et al.*, 2008].

[b]Data from total 111 Mesonet sites are available for the studied episode.

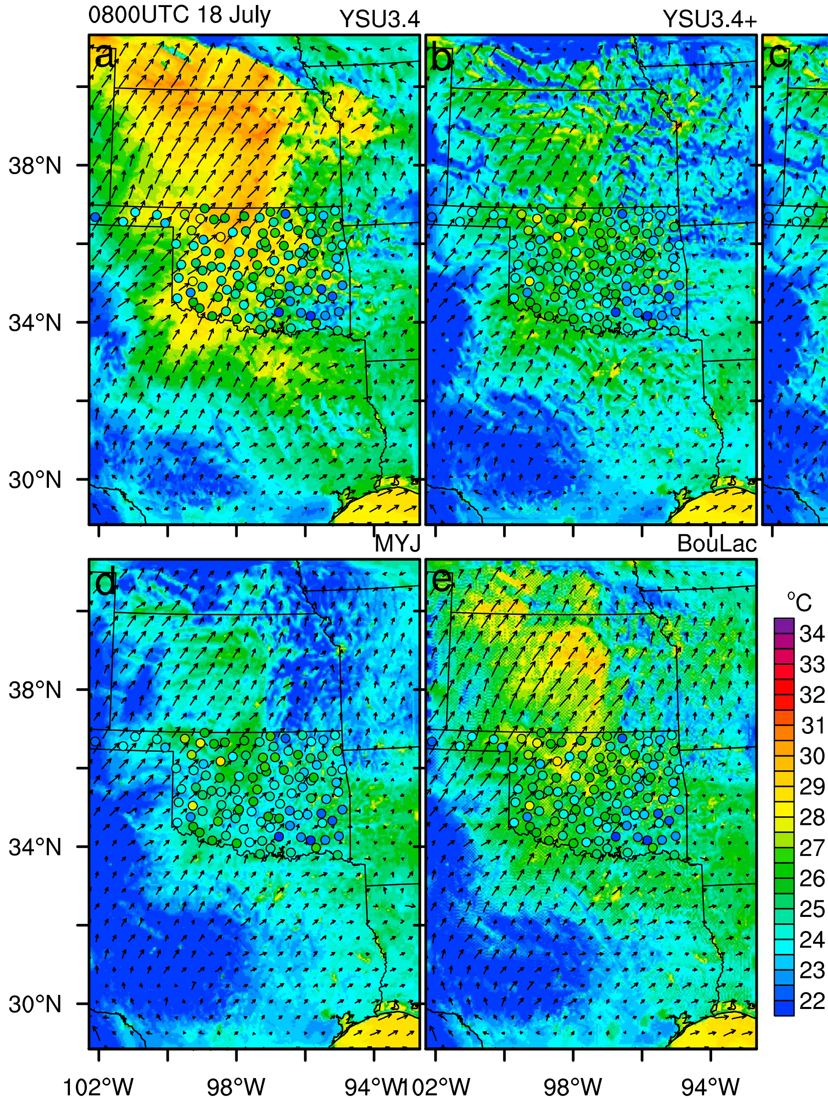

Figure 5. The 2 m temperature (T2) at 0800 UTC on 18 July 2003 simulated by the numerical experiments (a) YSU3.4, (b) YSU3.4+, (c) YSU3.4.1, (d) MYJ, and (e) BouLac. The observed values are indicated by shaded circles.

old YSU (i.e., 3.4) significantly overestimates the nighttime wind speeds with a mean bias (MB) of ~1.5 m s^{-1} and a normalized mean bias (NMB) of ~57% at all Mesonet sites (Table 2). This may indicate that the vertical coupling of horizontal momentum in the old YSU scheme is too strong during the simulated nighttime LLJ case, as was also pointed out by *Shin and Hong* [2011]. The excessive downward transport of momentum leads to the overestimation of near-surface wind speeds. The update to the YSU scheme in WRF 3.4.1 significantly improved the forecasting skill for the nighttime near-surface wind (NMB reduced to 12.6%, 10.8% for YSU3.4+, and YSU3.4.1, respectively) and did not affect the skill in daytime wind prediction. For the two experiments with other PBL schemes, BouLac overestimates nighttime wind speeds with a MB of 1.3 m s^{-1} and a NMB of 50.2%, while MYJ

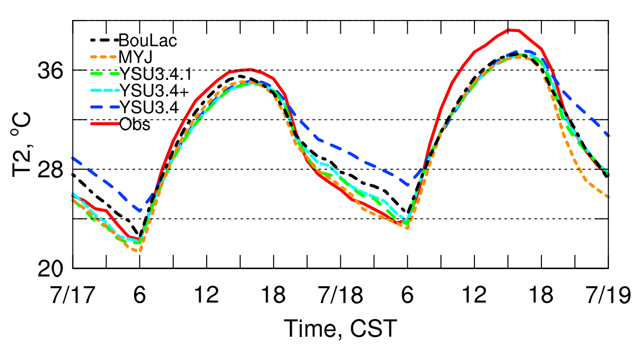

Figure 6. Observed and simulated average near-surface temperature (2 m AGL from simulations and 1.5 m from observations) at the six Mesonet sites around OKC.

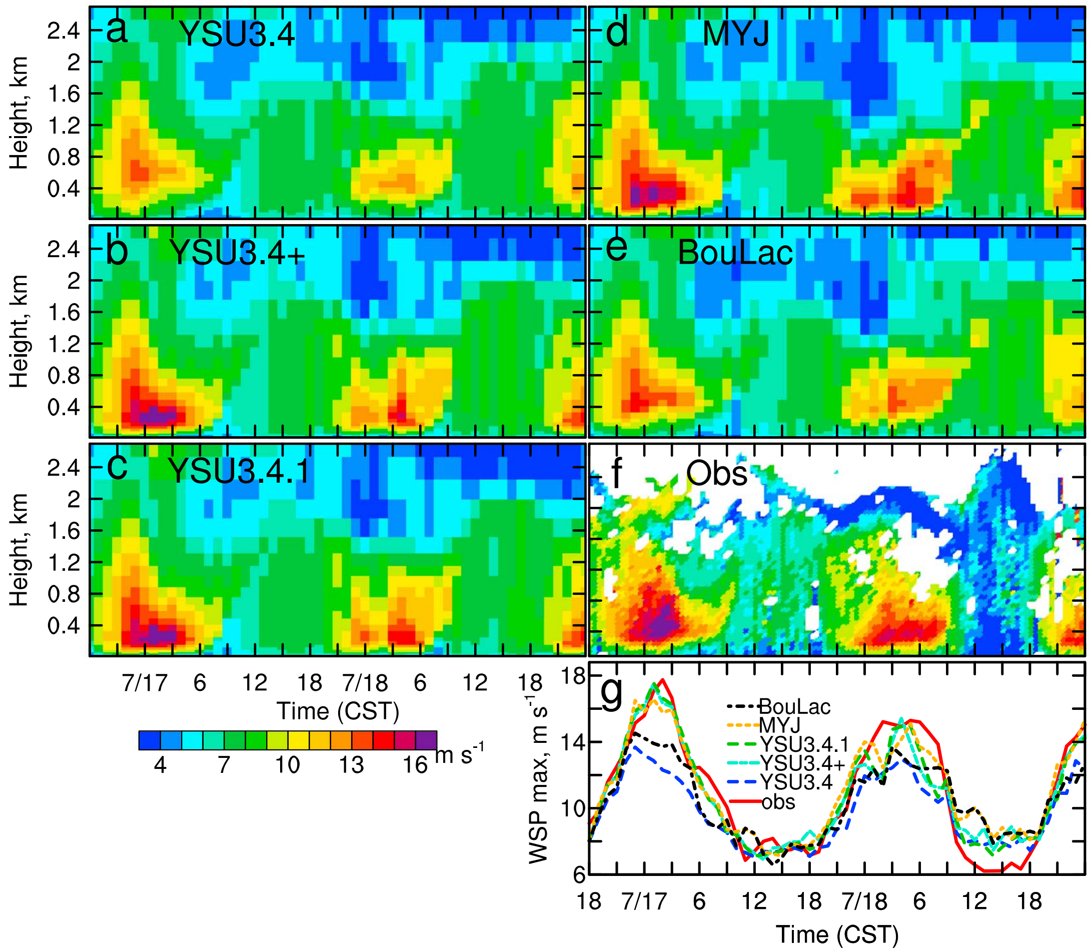

Figure 7. Time-height diagrams of wind speed at the ANL site simulated by the numerical experiments (a) YSU3.4, (b) YSU3.4+, (c) YSU3.4.1, (d) MYJ, and (e) BouLac and (f) observed by radar wind profiler, and (g) time series of observed and simulated maximum wind speed in the lower 2 km AGL. During the nighttime, the maximum wind speed is at the jet nose and it is defined as LLJ strength.

performs similar as YSU3.4+/YSU3.4.1 in terms of RMSE (1.3 m s^{-1}) but worse in terms of MB (0.7 m s^{-1}) and NMB (26.6%) (Table 2).

[16] Similar to near-surface winds (Figure 3), the WRF/Chem simulations with the updated YSU PBL scheme (i.e., YSU3.4+ and YSU3.4.1) show much better performance in predicting nighttime near-surface temperature than the YSU3.4 run (Figures 5, 6). The overestimation problem for the nighttime 2 m temperature (T2) for YSU3.4 (with a MB of 2.2 °C at 111 Mesonet sites in Oklahoma) is nearly eliminated in the other two simulations (with a MB of 0.05, 0.02°C for YSU3.4+ and YSU3.4.1 respectively, Table 2). BouLac also overestimates nighttime T2 by 0.7°C. Thus, BouLac has a similar, but less severe, problem as the old YSU scheme to overestimate nighttime near-surface wind speed and temperature. MYJ gives a cold bias during nighttime with a MB of −0.5 °C presumably due to insufficient vertical mixing [*Hu et al.*, 2010a]. All the simulations underestimate the daytime peak temperature (Figure 6), which might be due to other model errors (including the treatment of daytime boundary layer) and/or inaccuracy in model initial conditions (e.g., excessive soil moisture, [*Hu et al.*, 2010a]).

[17] Nocturnal LLJs are known to play important roles in modulating the nighttime boundary layer structure [*Hu et al.*, 2013a, 2013b]. In the presence of LLJs, strong shear on the underside of the jet often produces turbulent mixing that can propagate downward, even to the surface [*Smedman et al.*, 1993, 1995; *Banta et al.*, 2002, 2003; *Lundquist and Mirocha*, 2008; *Hu et al.*, 2013b]. In such cases, the turbulence in the boundary layer is generated aloft and not necessarily in significant communication with the surface. During these conditions, the boundary layers are called "upside-down" boundary layers [*Ha and Mahrt*, 2001; *Mahrt and Vickers*, 2002]. The development of nocturnal LLJs, documented by high-resolution radar wind profiler measurements (Figure 7f), is an interesting aspect of the selected study period. YSU3.4 successfully captures the occurrence of the nocturnal LLJs on each night (Figure 7a) but underestimates the LLJ strength by 3–4 m s^{-1} (Figure 7g). Underestimating the strength of LLJs was a longstanding problem for the WRF model with the YSU PBL scheme as recognized by a number of authors [*Storm et al.*, 2009; *Shin and Hong*, 2011; *Floors et al.*, 2013; *Schumacher et al.*, 2013]; but the exact cause was not clear to the authors. With the updated YSU PBL scheme,

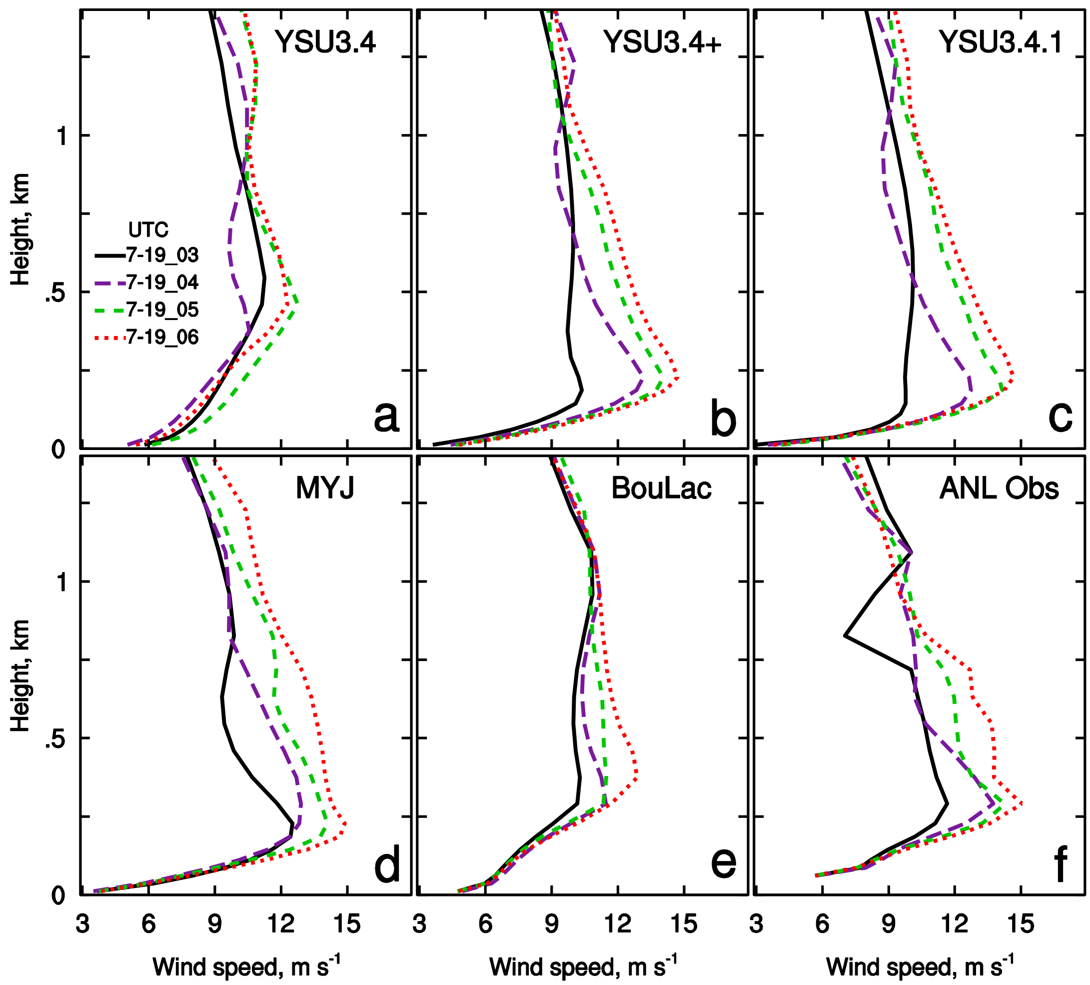

Figure 8. Wind profiles over the ANL site at 0300–0600 UTC on 19 July 2003 simulated by the numerical experiments (a) YSU3.4, (b) YSU3.4+, (c) YSU3.4.1, (d) MYJ, and (e) BouLac and (f) observed by the ANL radar wind profiler.

WRF/Chem simulates stronger LLJs (Figures 7b, 7c, 7g) that peak at lower levels, thus exhibiting a better agreement with the observations (Figure 7f) in terms of the LLJs maximum wind speeds as well as their elevations. BouLac shows a similar behavior as YSU3.4, simulating weaker and higher LLJs (Figures 7e, 7g), while the MYJ results are again very similar to YSU3.4.1 (Figures 7d, 7g).

[18] While wind profiles were measured continuously by the radar wind profiler at the ANL site during the study episode, temperature profiles were only measured by radiosondes released at the PNNL site at certain times during the night of 18–19 July [*De Wekker et al.*, 2004]. The simulated profiles of wind speed and temperature at those radiosonde release times are evaluated. In addition to the improvement seen in Figure 7, Figure 8 shows more clearly that the height of the jet nose is also in better agreement with observations for the simulations with the updated YSU PBL scheme (Figures 8b, 8c). The YSU3.4 simulation (Figure 8a) confirms the previously reported deficiencies of WRF predicting weaker and higher LLJs [*Storm et al.*, 2009; *Richardson*, 2012], likely caused by an overestimation of vertical mixing [*Storm et al.*, 2009; *Deppe*, 2011]. As seen in the comparison of eddy diffusivities from the simulations with the three WRF versions (Figures 9a, 9b, 9c), the updates in the YSU PBL scheme reduce the eddy diffusivities by a factor of nearly 10, and the new version limits the depth over which enhanced values occur. The artificially high eddy diffusivities in the old YSU scheme too strongly mix LLJ momentum toward the surface, resulting in underprediction of the LLJ strength (Figure 8a) and overprediction of near-surface wind speed (Figure 3a). Many PBL schemes implemented in numerical models artificially enhance vertical mixing in stable boundary layers to circumvent the "runaway cooling" problem (i.e., unrealistic cold bias near the surface, [*Beljaars and Holtslag*, 1991; *Viterbo et al.*, 1999; *Van de Wiel*, 2002; *Steeneveld et al.*, 2006; *Teixeira et al.*, 2008; *Hu et al.*, 2010a; *Grisogono*, 2010; *Atlaskin and Vihma*, 2012]). Likewise, the enhanced nighttime mixing in the older YSU scheme alleviated the near-surface cold bias problem [*Hu et al.*, 2010a] but at the expense of predicting too weak and too deep LLJs. Consequently, nighttime boundary layer height also tends to be overestimated with the older version of the YSU PBL scheme. Similar as YSU3.4, BouLac simulates weaker LLJs (Figure 8e), which is likely due to its overly strong vertical mixing in the nighttime boundary layer (Figure 9e). A tendency for overpredicting nighttime

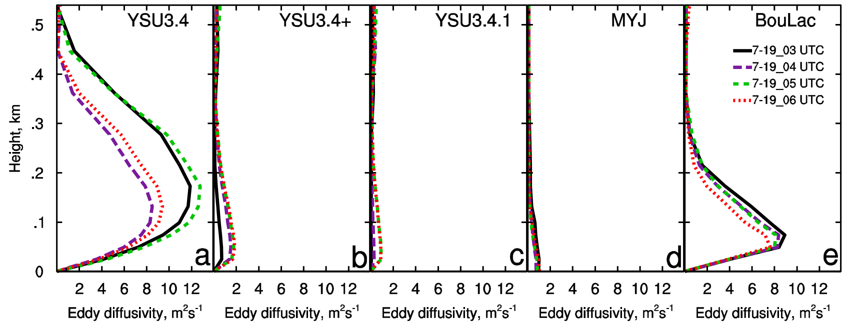

Figure 9. Vertical profiles of eddy diffusivity over the ANL site at 0300–0600 UTC on 19 July 2003 simulated by the numerical experiments (a) YSU3.4, (b) YSU3.4+, (c) YSU3.4.1, (d) MYJ, and (e) BouLac.

mixing with the BouLac scheme was also reported in *Bravo et al*. [2008].

[19] The artificially strong vertical mixing (illustrated by eddy diffusivities shown in Figure 9a) also affects the temperature structure resulting in an underprediction of nighttime near-surface inversion strength (Figure 10a). With the updated YSU PBL scheme, temperature profiles in the boundary layer compare better with the radiosonde observations, showing a more stable regime near the surface (Figures 10b, 10c). Due to its strong vertical mixing (Figure 9e), BouLac also simulates weaker stratification below 0.2 km AGL (Figure 10e) than the other PBL schemes. The vertical structure of the boundary layer plays an important role and should be carefully considered during model evaluation and improvement studies, while previous operational studies typically exclusively focused on near-surface variables [*Draxl et al*., 2012; *Sterk*

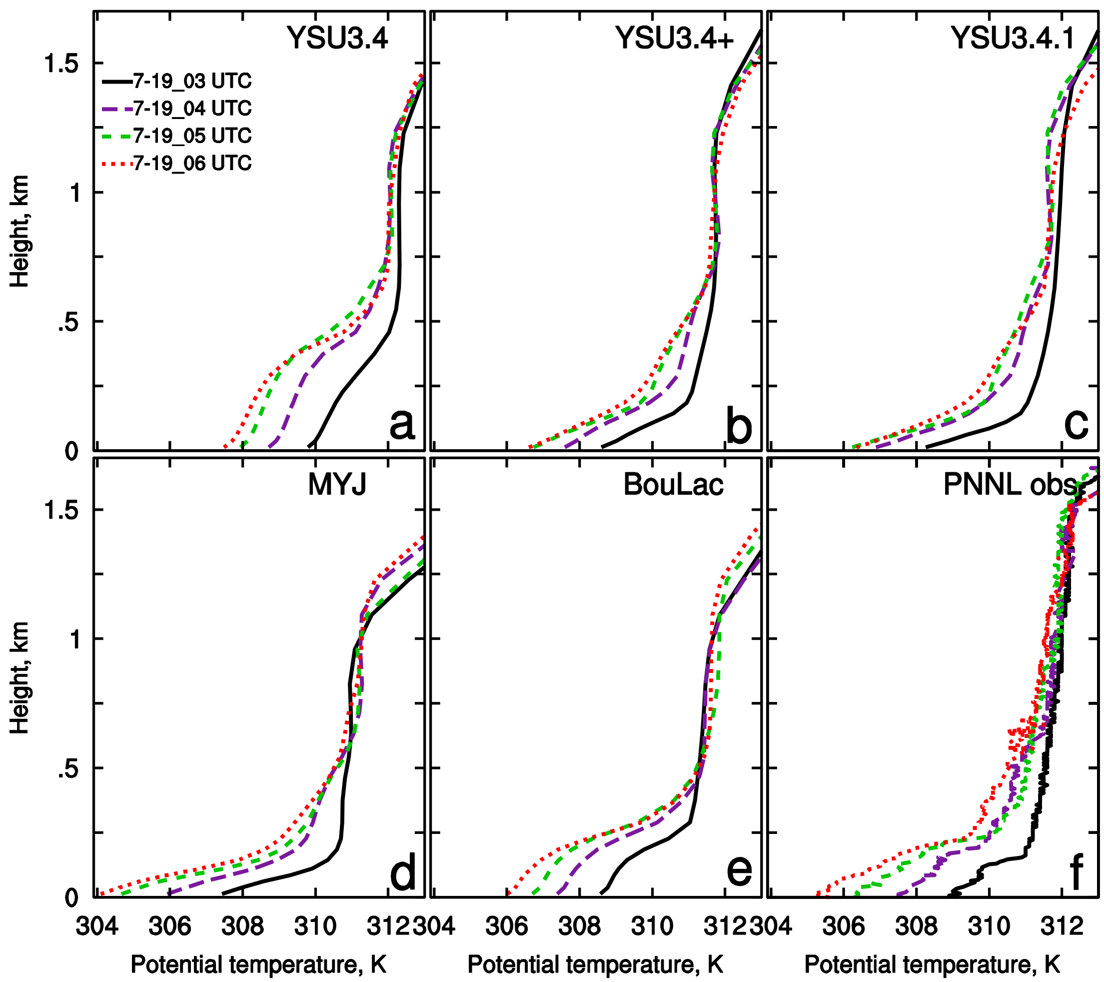

Figure 10. Profiles of potential temperature over the PNNL site at 0300–0600 UTC on 19 July 2003 simulated by the numerical experiments (a) YSU3.4, (b) YSU3.4+, (c) YSU3.4.1, (d) MYJ, and (e) BouLac, and (f) observed by radiosondes.

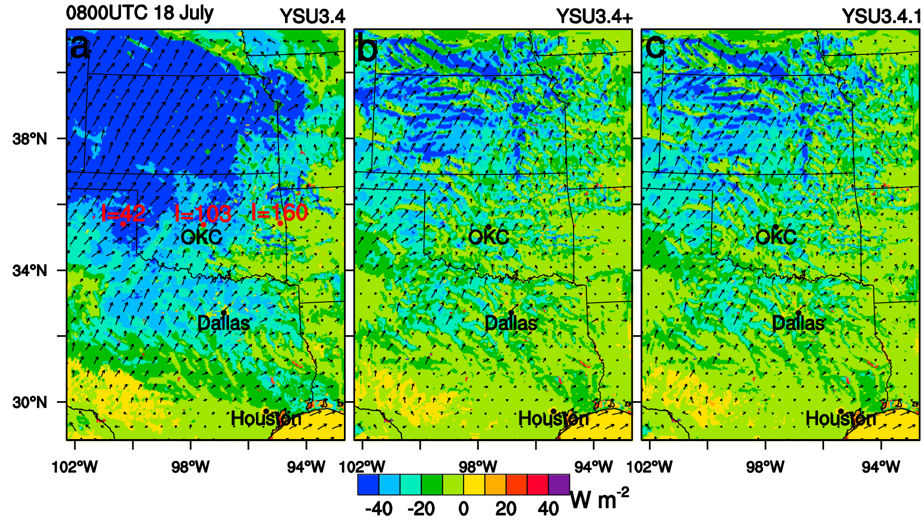

Figure 11. Spatial distribution of sensible heat flux (HFX) at 0800 UTC on 18 July 2003 simulated by the numerical experiments (a) YSU3.4, (b) YSU3.4+, and (c) YSU3.4.1. Three locations chosen for comparison in Figure 12 are marked in red.

et al., 2013; *Zhang et al.*, 2013]. An elevated inversion layer was observed at ~1.6 km AGL (Figure 10f). All five simulations capture this elevated inversion, but differences can be noted in the predicted strength and height of the inversion layer. During nighttime, vertical mixing at this altitude is suppressed and the elevated inversion is the remnant of the top boundary of the daytime CBL. Thus, strength and height of the simulated elevated inversion are affected by the treatment of the daytime CBL. The MYJ and BouLac schemes simulate a lower daytime PBL (figure not shown) due to their weaker daytime vertical mixing and weaker entrainment at the CBL top [*Hu et al.*, 2010; *LeMone et al.*, 2013]. Consequently, MYJ and BouLac predict the inversion layer at lower elevations (just above 1 km) (Figures 10d, 10e). All the schemes tend to underestimate the strength of the elevated inversion, which might be due to model uncertainties associated with vertical mixing in the residual layer and the free troposphere [*Hu et al.*, 2012] and/or insufficient vertical model resolution.

[20] Vertical mixing in the boundary layer also impacts the surface energy balances. The surface energy balances are of fundamental meteorological interest [*Steeneveld et al.*, 2006]. The updated YSU scheme predicts smaller downward sensible heat flux during the nighttime compared to the old version, especially in the area with stronger wind (e.g., in the northwestern part of domain 2, Figures 11b, 11c), due to weaker vertical mixing (Figures 9b, 9c). As a result, lower near-surface temperature is simulated, leading to a better agreement with the Mesonet observations (Figures 5b, 5c).

[21] The different impacts of the update to the YSU scheme in different regimes are a concern. On the night of 17–18 July 2003, the strength of the LLJ shows an east-to-west gradient (figure not shown). Such wind speed gradient associated with the LLJs over the Great Plains is also noticed in other studies [e.g., *Hu et al.*, 2013b], which is speculated to be related to the dynamics of the LLJs [*Wexler*, 1961]. The vertical wind profiles at three locations with different wind speeds (see Figure 11a for their locations) during this night are examined in Figure 12. For the OKC site and the site west of OKC (with stronger LLJs), the impact of the update of YSU is similar as that seen in Figure 8, i.e., WRF/Chem with the updated YSU predicts lower and stronger LLJs. For the site east of OKC (with weaker wind speeds), the difference predicted with the old and the updated YSU is diminished.

3.2. Prediction of the Boundary Layer Wind Profile Exponent

[22] Accurate predictions of near-surface wind shear are critical for wind resource assessment, short-term wind power forecasts, and wind-turbine design [*Storm et al.*, 2009; *Storm and Basu*, 2010]. For wind resource assessment, it is a common practice to use a power law relation like the following

$$U(z) = U_r \left(\frac{z}{z_r}\right)^{\alpha}, \tag{4}$$

to extrapolate the observed wind speed at a low level (typically 10 m) to turbine-hub heights (normally ~80 m) [*Storm et al.*, 2009; *Archer and Jacobson*, 2003]. In 4, U_r is the wind speed at a reference height (z_r) and $U(z)$ is the wind speed at height z above ground. In the past, the shear exponent, α, was often assumed to be $^1/_7$, but it is well-known that α varies with atmospheric stability as well as surface roughness [*Sisterson and Frenzen*, 1978; *Irwin*, 1979; *Storm et al.*, 2009; *Storm and Basu*, 2010].

[23] The average shear exponents between 10 m and ~82 m above the ground, estimated from different WRF/Chem simulations and the observations, are compared in Figure 13. For the hub-height observations, the wind speeds at the lowest level (82 m) detected by the radar wind profiler above the ANL site are used while the 10 m data are computed as the average value of observations at the six Mesonet sites around the OKC metro area. When the daytime wind speeds are relatively low, negative shear exponents are sometimes computed based on the average Mesonet 10 m wind speed and 82 m wind speed measured by the profiler at the ANL site, indicating that the average Mesonet 10 m wind speed is larger than the 82 m wind speed measured by the profiler at the ANL site. This may be due to two reasons: first, different

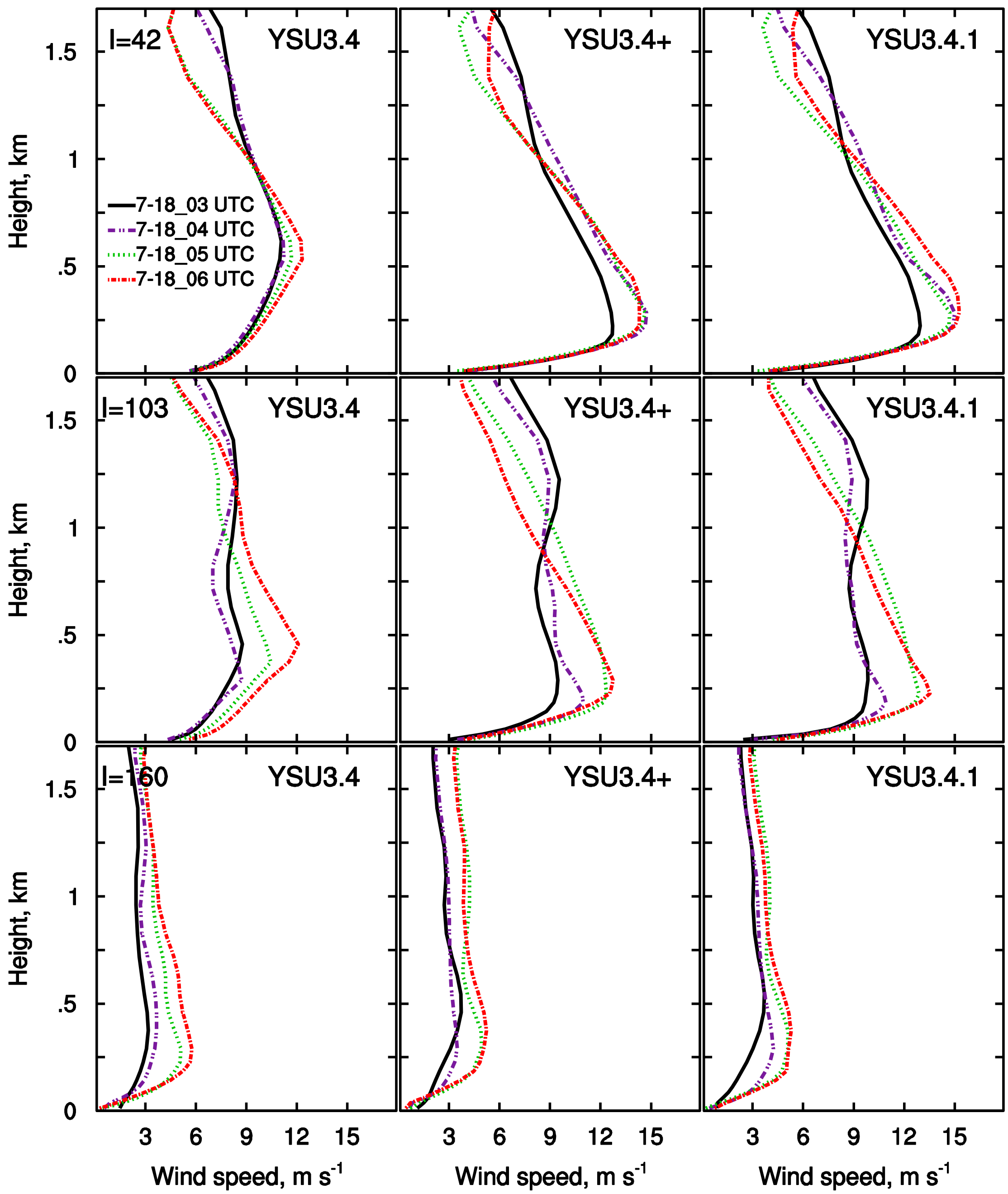

Figure 12. Vertical profiles of wind speed at 0300–0600 UTC on 18 July 2003 simulated by the numerical experiments (left column) YSU3.4, (middle column) YSU3.4+, and (right column) YSU3.4.1 at three locations (top to bottom). The three locations are marked in Figure 11a.

instrument errors from the Mesonet and the radar wind profiler; second, the wind speed at 82 m above the ANL site is different from the average wind speed at 82 m above the six Mesonet sites around the OKC metro area, likely due to the urban effects. Despite these issues, strong diurnal cycles of the shear exponent with much larger values (~0.4) at night than during the day can clearly be noted (Figure 13). Due to the diurnal variation of vertical coupling strength, i.e., strong coupling in daytime and weaker coupling at nighttime, the diurnal cycle of surface wind and wind at 82 m are out of phase, with the former exhibiting a maximum/minimum in the daytime/nighttime (Figure 4) in contrast to the latter showing a maximum/minimum in the nighttime/daytime (figure not shown). Such diurnal variations explain the diurnal cycles of the shear exponent.

[24] The YSU3.4 and BouLac simulations fail to reproduce the diurnal variation and significantly underestimate the nighttime shear exponents (Figure 13). The poor performance of YSU3.4 is consistent with the study of *Storm and Basu* [2010] and indicates that the old YSU scheme does not properly parameterize the vertically decoupled/weakly coupled flows at night. Similarly as MYJ, the YSU3.4+ and YSU3.4.1 simulations significantly improve the skill in predicting the shear exponent.

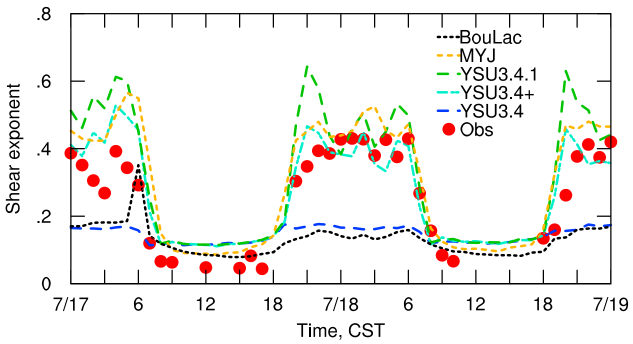

Figure 13. Observed and simulated average shear exponent at the ANL site.

3.3. Prediction of Near Surface O_3 Concentration

[25] The structure and dynamics of the nocturnal boundary layer also have important implications for the dispersion of pollutants; in the case of tropospheric O_3, the interplay between atmospheric chemistry and meteorology at night makes accurate forecasts particularly challenging [*Stutz et al.*, 2004; *Brown et al.*, 2007; *Ganzeveld et al.*, 2008; *Herwehe et al.*, 2011; *Hu et al.*, 2012, 2013a]. On the nights of 16–17 July and 17–18 July, surface O_3 at six EPA AQS sites in the OKC metro area were depleted to quite low levels (Figure 14f), which is typical for conditions with limited mixing between the surface and residual layer. Within the surface layer, the NO titration reaction and dry deposition cause the O_3 depletion, while the limited vertical mixing hinders both the upward transport of NO into the residual layer and the downward mixing of O_3. YSU3.4 overpredicts the nighttime minimum O_3 concentrations at most of the EPA sites (Figure 14a), while the updated YSU PBL scheme more accurately simulates the decreasing trend of O_3 concentrations in the early evening as well as the nighttime minimum O_3 concentration near the surface (Figures 14b, 14c). Such an improvement is consistent with the reduced vertical mixing associated with the updated YSU PBL scheme. Due to the O_3 removal processes near the surface, near-surface O_3 concentration is normally lower than that aloft at night. The stronger vertical mixing of the old YSU scheme replenishes near-surface O_3 by providing more downward transport of O_3-richer air (Figure 15a) while the updated scheme reduces this effect (Figures 15b, 15c). While improvement is achieved at most sites with the updated scheme, YSU3.4+ and YSU3.4.1 underpredict the nighttime minimum O_3 concentrations at particular sites (e.g., OKC). Note that during the night of 17–18 July, nighttime O_3 peaks are observed at a few sites (Figure 14f). These secondary nocturnal O_3 peaks are correlated with the onset of the LLJ as discussed by *Hu et al.* [2013a] and *Klein et al.* [2013], although at the same time, other processes including atmospheric chemistry, urban heat island circulations, and anthropogenic emissions also affect O_3 concentration. These processes are probably not accounted for in sufficient detail in our simulations and the updates of YSU in 3.4.1 do not necessarily always lead to a better performance of simulating the variation of nighttime O_3 concentrations (e.g., development of nighttime O_3 peaks). Note that in the current implementation of WRF/Chem, the turbulent diffusion coefficient is diagnosed in some PBL schemes (e.g., YSU, MYJ, MYNN2, BouLac, QNSE, and UW but not GFS, ACM2, and TEMF) and passed to a separate subroutine

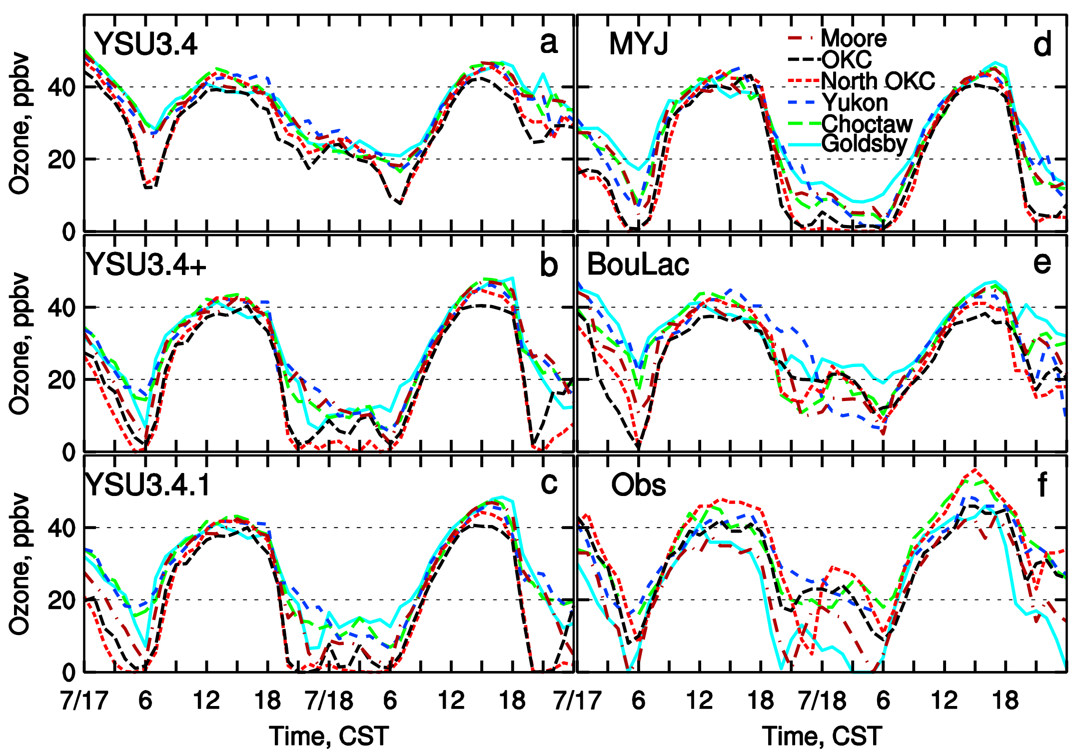

Figure 14. Time series of ozone at the six EPA sites in the Oklahoma City metropolitan area simulated by the numerical experiments (a) YSU3.4, (b) YSU3.4+, (c) YSU3.4.1, (d) MYJ, and (e) BouLac compared to (f) observations.

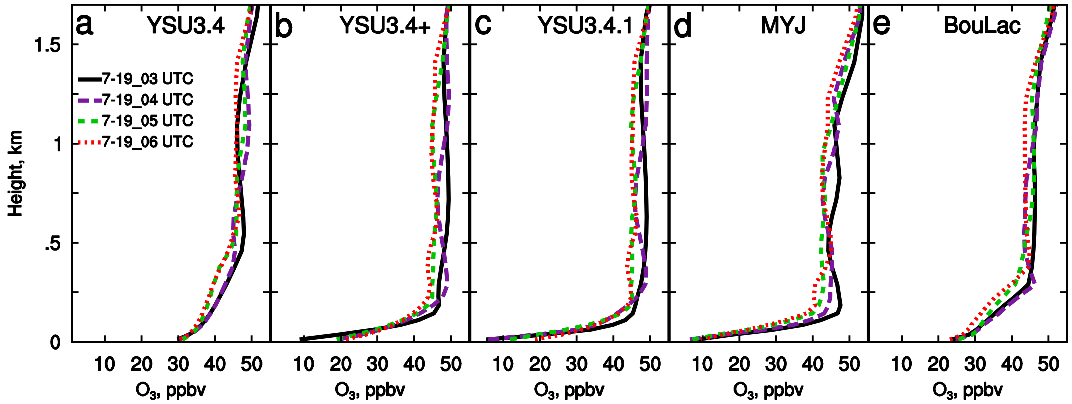

Figure 15. Vertical profiles of ozone over OKC at 0300–0600 UTC on 19 July 2003 simulated by the numerical experiments (a) YSU3.4, (b) YSU3.4+, (c) YSU3.4.1, (d) MYJ, and (e) BouLac.

to compute the vertical mixing of chemical species using a simple first-order closure scheme. As a result, only local mixing is considered while nonlocal mixing and entrainment processes are neglected for chemical species even though they are all considered for meteorological variables in some PBL schemes, e.g., YSU [*Hu et al*., 2012; *Pleim*, 2011]. Adding nonlocal mixing of chemical species in a global chemical-transport model appears to improve the vertical distribution of chemical species [*Lin and McElroy*, 2010]. Nonetheless, the strong impact of PBL vertical mixing on the skill of forecasting near-surface O_3 concentration is clearly demonstrated in this study (Figures 14, 15). Due to its strong vertical mixing at night, BouLac also predicts higher nighttime minimum O_3 on the night of 17–18 July than the updated YSU and MYJ PBL schemes (Figure 14e) and weaker vertical gradients of O_3 in the nighttime boundary layer (Figure 15e). Despite these facts, BouLac captures the secondary O_3 peaks on the night of 17–18 July reasonably well.

[26] All the schemes simulate the daytime maximum O_3 concentration reasonably well even though there are large model bias for meteorological variables during certain time periods (e.g., 1200–1800 CST 18 July, see Figures 4, 6). This is probably due to the fact that daytime O_3 concentration in this area is around regional average and photochemical production of O_3 is not intense. Thus O_3 simulation does not show much sensitivity to meteorological simulation during the daytime of this episode.

4. Summary and Discussions

[27] In version 3.4.1 of the WRF/Chem model, the previously erroneously formulated nighttime nondimensional profile function, ϕ_m, that appears in the vertical velocity scale ($w_s = u_*/\phi_m$) in the YSU PBL parameterization scheme is corrected. This correction significantly reduces the vertical velocity scale and the effective vertical turbulent mixing within nighttime boundary layer. The impacts of this update on the simulations of nighttime boundary layer wind and temperature structures, as well as air quality in terms of O_3 concentration, are investigated through three-dimensional WRF/Chem simulations over the southern Great Plains, for a period (0000 UTC 17 July–0600 UTC 19 July 2003) from the Joint Urban 2003 field experiment over the Oklahoma metropolitan area. The nighttime boundary layer flows during the period were characterized by LLJs on each night. Model simulations using the old and updated YSU PBL formulations are evaluated using surface measurements from the Oklahoma Mesonet sites and the EPA AQS sites as well as vertical profiles of wind and temperature obtained by a radar wind profiler and from radiosonde launched during the field experiment. Numerical experiments with WRF/Chem 3.4.1 with two other PBL schemes (i.e., MYJ, BouLac) are also conducted for comparison.

[28] With the reduced velocity scale, simulated nighttime vertical mixing strength is reduced, especially in the presence of strong wind shear. As a result, the prediction of boundary layer wind is much improved. The WRF model with the updated YSU scheme predicts stronger LLJs over the southern Great Plains with jet noses closer to the ground. The longstanding problem of the YSU PBL scheme's predicting too weak and too elevated LLJs appears to have been resolved with the fix. The predicted nighttime near-surface wind speeds are lower and in better agreement with observations, due to weaker coupling with stronger winds aloft. The improved prediction for boundary layer wind is significant for wind resource assessment. The shear exponent within the power law formulation commonly used in wind energy applications to extrapolate wind speed from a reference height is better simulated during nighttime with the updated YSU scheme. The thermal structure of the boundary layer is also improved, with the commonly observed problem of excessive nighttime vertical mixing alleviated, leading to a better agreement of surface temperature predictions with observations. The associated downward heat flux within the boundary layer is reduced. Due to the reduced vertical mixing, downward transport of O_3-richer air is also reduced, leading to improved predictions of the early evening decline of surface O_3 concentrations and the nighttime minimum O_3 concentration near the surface. However, deficiencies could still be noted in reproducing details in the O_3 variability at night (e.g., development of nighttime O_3 peak) with the current model configurations. For locations within the simulation domain where LLJ is weaker or absent, the impact of the YSU update is smaller. Among the two other PBL schemes tested, BouLac gives the strongest vertical mixing in the nighttime boundary layer, similar to the old YSU scheme. It consequently also overestimates

near-surface wind and temperature and underestimates the wind shear exponent at night. However, BouLac captures the nighttime secondary O_3 peaks reasonably well.

[29] In most previous model evaluation studies [e.g., *Berg and Zhong*, 2005; *Srinivas et al*., 2007; *Sanjay*, 2008; *Hu et al*., 2010a], PBL schemes are mostly evaluated for the "traditional" boundary layer, in which turbulence is generated at the surface and transported upward. There are very few comprehensive evaluations of PBL schemes for the "upside-down" boundary layer, in which turbulence is produced aloft and transported downward [*Todd et al*., 2008; *Carter et al*., 2011]. Further evaluation of model simulations with different PBL schemes, along with the collection of more suitable observations (e.g., turbulence profiles in the presence of LLJs), for the "upside-down" boundary layers is warranted for providing guidance to future model improvement [*Deppe*, 2011; *Deppe et al*., 2013; *Banta et al*., 2013].

[30] **Acknowledgments.** This work was supported by funding from the Office of the Vice President for Research at the University of Oklahoma. The second author was also supported through the NSF Career award ILREUM (NSF ATM 0547882). The third author was also supported by NSF grants OCI-0905040, AGS-0802888, AGS-0750790, AGS-0941491, AGS-1046171, and AGS-1046081. Computations were performed at the Texas Advanced Computing Center (TACC). Discussion with Songyou Hong helped to confirm the code updates from WRF versions 3.4 to 3.4.1. Proofreading by David C. Doughty is greatly appreciated. Four anonymous reviewers provided helpful comments that improved the manuscript.

References

Archer, C. L., and M. Z. Jacobson (2003), Spatial and temporal distributions of US winds and wind power at 80 m derived from measurements, *J. Geophys. Res.*, *108*(D9), 4289, doi:10.1029/2002JD002076.

Arnold, J. R., and R. L. Dennis (2001), First results from operational testing of the U.S. EPA Models-3/Community Multiscale Model for Air Quality (CMAQ), in *Air Pollution Modeling and Its Application XIV*, edited by S.-E. Gryning and F. A. Schiermeier, pp. 651–658, Kluwer Acad., Norwell, Mass.

Atlaskin, E., and T. Vihma (2012), Evaluation of NWP results for wintertime nocturnal boundary layer temperatures over Europe and Finland, *Q. J. Roy Meteor. Soc.*, *138*(667), 1440–1451, doi:10.1002/Qj.1885.

Banta, R. M., R. K. Newsom, J. K. Lundquist, Y. L. Pichugina, R. L. Coulter, and L. Mahrt (2002), Nocturnal low-level jet characteristics over Kansas during CASES-99, *Bound-Lay Meteorol.*, *105*(2), 221–252, doi:10.1023/A:1019992330866.

Banta, R. M., Y. L. Pichugina, and R. K. Newsom (2003), Relationship between low-level jet properties and turbulence kinetic energy in the nocturnal stable boundary layer, *J. Atmos. Sci.*, *60*(20), 2549–2555, doi:10.1175/1520-0469(2003)060<2549:Rbljpa>2.0.Co;2.

Banta, R. M., Y. L. Pichugina, N. D. Kelley, R. M. Hardesty, and W. A. Brewer (2013), Wind Energy Meteorology: Insight into wind properties in the turbine-rotor layer of the atmosphere from high-resolution doppler lidar, *Bull. Am. Meteorol. Soc.*, *94*(6), 883–902, doi:10.1175/Bams-D-11-00057.1.

Bao, J. W., S. A. Michelson, P. O. G. Persson, I. V. Djalalova, and J. M. Wilczak (2008), Observed and WRF-simulated low-level winds in a high-ozone episode during the Central California Ozone Study, *J. Appl. Meteorol. Climatol.*, *47*(9), 2372–2394, doi:10.1175/2008jamc1822.1.

Beare, R. J., et al. (2006), An intercomparison of large-eddy simulations of the stable boundary layer, *Bound-Lay Meteorol.*, *118*(2), 247–272, doi:10.1007/s10546-004-2820-6.

Beljaars, A. C. M., and A. A. M. Holtslag (1991), Flux Parameterization over Land Surfaces for Atmospheric Models, *J. Appl. Meteorol.*, *30*(3), 327–341, doi:10.1175/1520-0450(1991)030<0327:Fpolsf>2.0.Co;2.

Berg, L. K., and S. Y. Zhong (2005), Sensitivity of MM5-simulated boundary layer characteristics to turbulence parameterizations, *J. Appl. Meteorol.*, *44*(9), 1467–1483, doi:10.1175/Jam2292.1.

Borge, R., V. Alexandrov, J. J. del Vas, J. Lumbreras, and E. Rodriguez (2008), A comprehensive sensitivity analysis of the WRF model for air quality applications over the Iberian Peninsula, *Atmos. Environ.*, *42*(37), 8560–8574, doi:10.1016/j.atmosenv.2008.08.032.

Bougeault, P., and P. Lacarrere (1989), Parameterization of orography-induced turbulence in a mesobeta-scale model, *Mon. Weather Rev.*, *117*(8), 1872–1890, doi:10.1175/1520-0493(1989)117<1872:Pooiti>2.0.Co;2.

Bravo, M., T. Mira, M. R. Soler, and J. Cuxart (2008), Intercomparison and evaluation of MM5 and Meso-NH mesoscale models in the stable boundary layer, *Bound-Lay Meteorol.*, *128*(1), 77–101, doi:10.1007/s10546-008-9269-y.

Brost, R. A., and J. C. Wyngaard (1978), A model study of the stably stratified planetary boundary layer, *J. Atmos. Sci.*, *35*(8), 1427–1440, doi:10.1175/1520-0469(1978)035<1427:amsots>2.0.co;2.

Brown, S. S., W. P. Dubé, H. D. Osthoff, D. E. Wolfe, W. M. Angevine, and A. R. Ravishankara (2007), High resolution vertical distributions of NO_3 and N_2O_5 through the nocturnal boundary layer, *Atmos. Chem. Phys.*, *7*(1), 139–149, doi:10.5194/acp-7-139-2007.

Brown, A. R., R. J. Beare, J. M. Edwards, A. P. Lock, S. J. Keogh, S. F. Milton, and D. N. Walters (2008), Upgrades to the boundary layer scheme in the Met Office numerical weather prediction model, *Bound-Lay Meteorol.*, *128*(1), 117–132, doi:10.1007/s10546-008-9275-0.

Carter, K. C., A. J. Deppe, and W. A. Gallus (2011), Simulations of nocturnal LLJs with a WRF PBL scheme ensemble and comparison to observations from the ARM project. 20th Conf. on Numerical Weather Prediction, Seattle, WA, Amer. Meteor. Soc. P474.

Carvalho, D., A. Rocha, M. Gomez-Gesteira, and C. Santos (2012), A sensitivity study of the WRF model in wind simulation for an area of high wind energy, *Environ. Modell. Software*, *33*, 23–34, doi:10.1016/j.envsoft.2012.01.019.

Chen, F., and J. Dudhia (2001), Coupling an advanced land surface-hydrology model with the Penn State-NCAR MM5 modeling system. Part I: Model implementation and sensitivity, *Mon. Weather Rev.*, *129*(4), 569–585, doi:10.1175/1520-0493(2001)129<0569:Caalsh>2.0.Co;2.

Chen, J. J., H. T. Mao, R. W. Talbot, and R. J. Griffin (2006), Application of the CACM and MPMPO modules using the CMAQ model for the eastern United States, *J. Geophys. Res.*, *111*, D23S25, doi:10.1029/2006JD007603.

Chen, J., J. Vaughan, J. Avise, S. O'Neill, and B. Lamb (2008), Enhancement and evaluation of the AIRPACT ozone and $PM_{2.5}$ forecast system for the Pacific Northwest, *J. Geophys. Res.*, *113*, D14305, doi:10.1029/2007JD009554.

Cheng, F. Y., S. C. Chin, and T. H. Liu (2012), The role of boundary layer schemes in meteorological and air quality simulations of the Taiwan area, *Atmos. Environ.*, *54*, 714–727, doi:10.1016/j.atmosenv.2012.01.029.

Coniglio, M. C., J. Correia, P. T. Marsh, and F. Kong (2013), Verification of convection-allowing WRF model forecasts of the planetary boundary layer using sounding observations, *Weather Forecast*, *28*(3), 842–862, doi:10.1175/Waf-D-12-00103.1.

De Wekker, S. F. J., L. K. Berg, J. Allwine, J. C. Doran, and W. J. Shaw (2004), Boundary-layer structure upwind and downwind of Oklahoma City during the Joint Urban 2003 field study. Preprints. Fifth Conf. on Urban Environment, Vancouver, BC, Canada, Amer. Meteor. Soc., CD-ROM, 3.20.

Deppe, A. J. (2011), Improvements in numerical prediction of low level winds. Graduate Theses and Dissertations. Paper 10100. http://lib.dr.iastate.edu/etd/10100.

Deppe, A. J., W. A. Gallus, and E. S. Takle (2013), A WRF ensemble for improved wind speed forecasts at turbine height, *Weather Forecast*, *28*(1), 212–228, doi:10.1175/WAF-D-11-00112.1.

Draxl, C., A. N. Hahmann, A. Peña, and G. Giebel (2012), Evaluating winds and vertical wind shear from Weather Research and Forecasting model forecasts using seven planetary boundary layer schemes, *Wind Energy*, doi:10.1002/we.1555.

Dudhia, J. (1989), Numerical study of convection observed during the winter monsoon experiment using a mesoscale two-dimensional model, *J. Atmos. Sci.*, *46*(20), 3077–3107, doi:10.1175/1520-0469(1989)046<3077:Nsocod>2.0.Co;2.

Eder, B., D. W. Kang, R. Mathur, S. C. Yu, and K. Schere (2006), An operational evaluation of the Eta-CMAQ air quality forecast model, *Atmos. Environ.*, *40*(26), 4894–4905, doi:10.1016/j.atmonsenv.2005.12.062.

Emmons, L. K., et al. (2010), Description and evaluation of the Model for Ozone and Related Chemical Tracers, version 4 (MOZART-4), *Geosci. Model Dev.*, *3*(1), 43–67, doi:10.5194/gmd-3-43-2010.

Engardt, M. (2008), Modelling of near-surface ozone over South Asia, *J. Atmos. Chem.*, *59*(1), 61–80, doi:10.1007/s10874-008-9096-z.

Fernando, H. J. S., and J. C. Weil (2010), Whither the stable boundary layer? A shift in the research agenda, *Bull. Am. Meteorol. Soc.*, *91*(11), 1475–1484, doi:10.1175/2010bams2770.1.

Fiebrich, C. A., and K. C. Crawford (2001), The impact of unique meteorological phenomena detected by the Oklahoma Mesonet and ARS Micronet on automated quality control, *Bull. Am. Meteorol. Soc.*, *82*(10), 2173–2187, doi:10.1175/1520-0477(2001)082<2173:Tioump>2.3.Co;2.

Floors, R., C. L. Vincent, S. E. Gryning, A. Peña, and E. Batchvarova (2013), The wind profile in the coastal boundary layer: Wind lidar measurements and numerical modelling, *Bound-Lay Meteorol.*, *147*(3), 469–491, doi:10.1007/s10546-012-9791-9.

Ganzeveld, L., et al. (2008), Surface and boundary layer exchanges of volatile organic compounds, nitrogen oxides and ozone during the GABRIEL campaign, *Atmos. Chem. Phys.*, *8*(20), 6223–6243, doi:10.5194/acp-8-6223-2008.

García-Díez, M., J. Fernández, L. Fita, and C. Yagüe (2013), Seasonal dependence of WRF model biases and sensitivity to PBL schemes over Europe, *Quart. J. Roy. Meteor. Soc.*, *139*(671), 501–514, doi:10.1002/qj.1976.

Garcia-Menendez, F., Y. Hu, and M. T. Odman (2013), Simulating smoke transport from wildland fires with a regional-scale air quality model: Sensitivity to uncertain wind fields, *J Geophys Res. Atmos*, *118*, 6493–6504, doi:10.1002/jgrd.50524.

Gilliam, R. C., and J. E. Pleim (2010), Performance assessment of new land surface and planetary boundary layer physics in the WRF-ARW, *J. Appl. Meteorol. Climatol.*, *49*(4), 760–774, doi:10.1175/2009jamc2126.1.

Gilliam, R. C., J. M. Godowitch, and S. T. Rao (2012), Improving the horizontal transport in the lower troposphere with four dimensional data assimilation, *Atmos. Environ.*, *53*, 186–201, doi:10.1016/j.atmosenv.2011.10.064.

Grell, G. A., S. E. Peckham, R. Schmitz, S. A. McKeen, G. Frost, W. C. Skamarock, and B. Eder (2005), Fully coupled "online" chemistry within the WRF model, *Atmos. Environ.*, *39*(37), 6957–6975, doi:10.1016/j.atmosenv.2005.04.027.

Grisogono, B. (2010), Generalizing 'z-less' mixing length for stable boundary layers, *Quart. J. Roy. Meteor. Soc.*, *136*(646), 213–221, doi:10.1002/Qj.529.

Grisogono, B., and D. Belusic (2008), Improving mixing length-scale for stable boundary layers, *Quart. J. Roy. Meteor. Soc.*, *134*(637), 2185–2192, doi:10.1002/Qj.347.

Guenther, A., P. Zimmerman, and M. Wildermuth (1994), Natural volatile organic-compound emission rate estimates for United-States woodland landscapes, *Atmos. Environ.*, *28*(6), 1197–1210, doi:10.1016/1352-2310(94)90297-6.

Ha, K. J., and L. Mahrt (2001), Simple inclusion of z-less turbulence within and above the modeled nocturnal boundary layer, *Mon. Weather Rev.*, *129*(8), 2136–2143, doi:10.1175/1520-0493(2001)129<2136:Siozlt>2.0.Co;2.

Han, Z. W., H. Ueda, and J. L. An (2008), Evaluation and intercomparison of meteorological predictions by five MM5-PBL parameterizations in combination with three land-surface models, *Atmos. Environ.*, *42*(2), 233–249, doi:10.1016/j.atmosenv.2007.09.053.

Hanna, S. R., and R. X. Yang (2001), Evaluations of mesoscale models' simulations of near-surface winds, temperature gradients, and mixing depths, *J. Appl. Meteorol.*, *40*(6), 1095–1104, doi:10.1175/1520-0450(2001)040<1095:Eommso>2.0.Co;2.

Herwehe, J. A., T. L. Otte, R. Mathur, and S. T. Rao (2011), Diagnostic analysis of ozone concentrations simulated by two regional-scale air quality models, *Atmos. Environ.*, *45*(33), 5957–5969, doi:10.1016/j.atmosenv.2011.08.011.

Hong, S. Y. (2010), A new stable boundary layer mixing scheme and its impact on the simulated East Asian summer monsoon, *Quart. J. Roy. Meteor. Soc.*, *136*(651), 1481–1496, doi:10.1002/Qj.665.

Hong, S. Y., J. Dudhia, and S. H. Chen (2004), A revised approach to ice microphysical processes for the bulk parameterization of clouds and precipitation, *Mon. Weather Rev.*, *132*(1), 103–120, doi:10.1175/1520-0493(2004)132<0103:Aratim>2.0.Co;2.

Hong, S. Y., Y. Noh, and J. Dudhia (2006), A new vertical diffusion package with an explicit treatment of entrainment processes, *Mon. Weather Rev.*, *134*(9), 2318–2341, doi:10.1175/Mwr3199.1.

Hu, X.-M. (2008), Incorporation of the Model of Aerosol Dynamics, Reaction, Ionization, and Dissolution (MADRID) into the Weather Research and Forecasting Model with Chemistry (WRF/Chem): Model development and retrospective applications, Ph.D. dissertation, N. C. State Univ., Raleigh, July. http://repository.lib.ncsu.edu/ir/handle/1840.16/5241.

Hu, X.-M., J. W. Nielsen-Gammon, and F. Q. Zhang (2010a), Evaluation of three planetary boundary layer schemes in the WRF model, *J. Appl. Meteorol. Climatol.*, *49*(9), 1831–1844, doi:10.1175/2010jamc2432.1.

Hu, X.-M., F. Q. Zhang, and J. W. Nielsen-Gammon (2010b), Ensemble-based simultaneous state and parameter estimation for treatment of mesoscale model error: A real-data study, *Geophys. Res. Lett.*, *37*, L08802, doi:10.1029/2010GL043017.

Hu, X.-M., J. D. Fuentes, and F. Q. Zhang (2010c), Downward transport and modification of tropospheric ozone through moist convection, *J. Atmos. Chem.*, *65*(1), 13–35, doi:10.1007/s10874-010-9179-5.

Hu, X.-M., D. C. Doughty, K. J. Sanchez, E. Joseph, and J. D. Fuentes (2012), Ozone variability in the atmospheric boundary layer in Maryland and its implications for vertical transport model, *Atmos. Environ.*, *46*, 354–364, doi:10.1016/j.atmosenv.2011.09.054.

Hu, X.-M., P. M. Klein, M. Xue, F. Q. Zhang, D. C. Doughty, R. Forkel, E. Joseph, and J. D. Fuentes (2013a), Impact of the vertical mixing induced by low-level jets on boundary layer ozone concentration, *Atmos. Environ.*, *70*, 123–130, doi:10.1016/j.atmosenv.2012.12.046.

Hu, X.-M., P. M. Klein, M. Xue, J. K. Lundquist, F. Zhang, and Y. Qi (2013b), Impact of low-level jets on the nocturnal urban heat island intensity in Oklahoma City, *J. Appl. Meteorol. Climatol.*, *52*(8), 1779–1802, doi:10.1175/Jamc-D-12-0256.1.

Hu, X.-M., P. M. Klein, M. Xue, A. Shapiro, and A. Nallapareddy (2013c), Enhanced vertical mixing associated with a nocturnal cold front passage and its impact on near-surface temperature and ozone concentration, *J. Geophys. Res. Atmos.*, *118*, 2714–2728, doi:10.1002/jgrd.50309.

Irwin, J. S. (1979), Theoretical variation of the wind profile power-law exponent as a function of surface-roughness and stability, *Atmos. Environ.*, *13*(1), 191–194, doi:10.1016/0004-6981(79)90260-9.

Janjic, Z. I. (1990), The step-mountain coordinate: Physical package, *Mon. Weather Rev.*, *118*(7), 1429–1443, doi:10.1175/1520-0493(1990)118<1429:Tsmcpp>2.0.Co;2.

Jankov, I., W. A. Gallus, M. Segal, B. Shaw, and S. E. Koch (2005), The impact of different WRF model physical parameterizations and their interactions on warm season MCS rainfall, *Weather Forecast*, *20*(6), 1048–1060, doi:10.1175/Waf888.1.

Jankov, I., P. J. Schultz, C. J. Anderson, and S. E. Koch (2007), The impact of different physical parameterizations and their interactions on cold season QPF in the American River basin, *J. Hydrometeorol.*, *8*(5), 1141–1151, doi:10.1175/Jhm630.1.

Klein, P. M., X.-M. Hu, and M. Xue (2013), Impacts of mixing processes in the nocturnal atmospheric boundary layer on urban ozone concentrations, *Bound-Lay Meteorol.*, doi:10.1007/s10546-013-9864-4.

Kolling, J. S., J. E. Pleim, H. E. Jeffries, and W. Vizuete (2012), A multisensor evaluation of the Asymmetric Convective Model, Version 2, in southeast Texas, *J. Air Waste Manage.*, *63*(1), 41–53, doi:10.1080/10962247.2012.732019.

Lareau, N. P., E. Crosman, C. D. Whiteman, J. D. Horel, S. W. Hoch, W. O. J. Brown, and T. W. Horst (2013), The persistent cold-air pool study, *Bull. Am. Meteorol. Soc.*, *94*(1), 51–63, doi:10.1175/Bams-D-11-00255.1.

LeMone, M. A., M. Tewari, F. Chen, and J. Dudhia (2013), Objectively determined fair-weather CBL depths in the ARW-WRF model and their comparison to CASES-97 observations, *Mon. Weather Rev.*, *141*(1), 30–54, doi:10.1175/Mwr-D-12-00106.1.

Li, X. L., and Z. X. Pu (2008), Sensitivity of numerical simulation of early rapid intensification of hurricane emily (2005) to cloud microphysical and planetary boundary layer parameterizations, *Mon. Weather Rev.*, *136*(12), 4819–4838, doi:10.1175/2008mwr2366.1.

Lin, J. T., and M. B. McElroy (2010), Impacts of boundary layer mixing on pollutant vertical profiles in the lower troposphere: Implications to satellite remote sensing, *Atmos. Environ.*, *44*(14), 1726–1739, doi:10.1016/j.atmosenv.2010.02.009.

Lundquist, J. K., and J. D. Mirocha (2008), Interaction of nocturnal low-level jets with urban geometries as seen in joint urban 2003 data, *J. Appl. Meteorol. Climatol.*, *47*(1), 44–58, doi:10.1175/2007jamc1581.1.

Mahrt, L., and D. Vickers (2002), Contrasting vertical structures of nocturnal boundary layers, *Bound-Lay Meteorol.*, *105*(2), 351–363, doi:10.1023/A:1019964720989.

Mao, Q., L. L. Gautney, T. M. Cook, M. E. Jacobs, S. N. Smith, and J. J. Kelsoe (2006), Numerical experiments on MM5-CMAQ sensitivity to various PBL schemes, *Atmos. Environ.*, *40*(17), 3092–3110, doi:10.1016/j.atmosenv.2005.12.055.

McPherson, R. A., et al. (2007), Statewide monitoring of the mesoscale environment: A technical update on the Oklahoma Mesonet, *J. Atmos. Oceanic Technol.*, *24*(3), 301–321, doi:10.1175/Jtech1976.1.

Mebust, M. R., B. K. Eder, F. S. Binkowski, and S. J. Roselle (2003), Models-3 community multiscale air quality (CMAQ) model aerosol component - 2. Model evaluation, *J. Geophys. Res.*, *108*(D6), 4184, doi:10.1029/2001JD001410.

Miao, J. F., D. Chen, K. Wyser, K. Borne, J. Lindgren, M. K. S. Strandevall, S. Thorsson, C. Achberger, and E. Almkvist (2008), Evaluation of MM5 mesoscale model at local scale for air quality applications over the Swedish west coast: Influence of PBL and LSM parameterizations, *Meteor. Atmos. Phys.*, *99*(1–2), 77–103, doi:10.1007/s00703-007-0267-2.

Mlawer, E. J., S. J. Taubman, P. D. Brown, M. J. Iacono, and S. A. Clough (1997), Radiative transfer for inhomogeneous atmospheres: RRTMa validated correlated-k model for the longwave, *J. Geophys. Res.*, *102*(D14), 16,663–16,682, doi:10.1029/97JD00237.

Mohan, M., and S. Bhati (2011), Analysis of WRF model performance over subtropical region of Delhi, India, *Adv Meteorol.*, doi:10.1155/2011/621235.

Nielsen-Gammon, J. W., X. M. Hu, F. Q. Zhang, and J. E. Pleim (2010), Evaluation of planetary boundary layer scheme sensitivities for the purpose of parameter estimation, *Mon. Weather Rev.*, *138*(9), 3400–3417, doi:10.1175/2010mwr3292.1.

Pleim, J. E. (2007a), A combined local and nonlocal closure model for the atmospheric boundary layer. Part I: Model description and testing, *J. Appl. Meteorol. Climatol.*, *46*(9), 1383–1395, doi:10.1175/Jam2539.1.

Pleim, J. E. (2007b), A combined local and nonlocal closure model for the atmospheric boundary layer, Part II: Application and evaluation in a mesoscale meteorological model, *J. Appl. Meteorol. Climatol.*, *46*(9), 1396–1409, doi:10.1175/Jam2534.1.

Pleim, J. E. (2011), Comment on "Simulation of surface ozone pollution in the central gulf coast region using WRF/Chem model: Sensitivity to PBL and land surface physics", *Adv. Meteorol.*, 464753, doi:10.1155/2011/464753.

Prabha, T., and G. Hoogenboom (2008), Evaluation of the Weather Research and Forecasting model for two frost events, *Comput Electron Agr*, *64*(2), 234–247, doi:10.1016/j.compag.2008.05.019.

Prabha, T. V., G. Hoogenboom, and T. G. Smirnova (2011), Role of land surface parameterizations on modeling cold-pooling events and low-level jets, *Atmos Res*, *99*(1), 147–161, doi:10.1016/j.atmosres.2010.09.017.

Richardson, H. L. (2012), Improving stable boundary layer parameterization in a mesoscale model to better represent nocturnal low-level jets, M.S. thesis, N. C. State Univ., Raleigh, July. http://www.lib.ncsu.edu/resolver/1840.16/7948.

Salmond, J. A., and I. G. McKendry (2005), A review of turbulence in the very stable nocturnal boundary layer and its implications for air quality, *Prog. Phys. Geogr.*, *29*(2), 171–188, doi:10.1191/0309133305pp442ra.

Sanjay, J. (2008), Assessment of atmospheric boundary-layer processes represented in the numerical model MM5 for a clear sky day using LASPEX observations, *Bound-Lay Meteorol.*, *129*(1), 159–177, doi:10.1007/s10546-008-9298-6.

Schumacher, R. S., A. J. Clark, M. Xue, and F. Kong (2013), Factors influencing the development and maintenance of nocturnal heavy-rain-producing convective systems in a storm-scale ensemble, *Mon. Weather Rev.*, *141*(8), 2778–2801, doi:10.1175/Mwr-D-12-00239.1.

Seigneur, C., et al. (2000), Guidance for the performance evaluation of three-dimensional air quality modeling systems for particulate matter and visibility, *J. Air Waste Manage.*, *50*(4), 588–599.

Shimada, S., T. Ohsawa, S. Chikaoka, and K. Kozai (2011), Accuracy of the wind speed profile in the lower PBL as simulated by the WRF model, *Sola*, *7*, 109–112, doi:10.2151/sola.2011-028.

Shin, H. H., and S. Y. Hong (2011), Intercomparison of planetary boundary-layer parametrizations in the WRF model for a single day from CASES-99, *Bound-Lay Meteorol.*, *139*(2), 261–281, doi:10.1007/s10546-010-9583-z.

Sisterson, D. L., and P. Frenzen (1978), Nocturnal boundary-layer wind maxima and problem of wind power assessment, *Environ. Sci. Technol.*, *12*(2), 218–221, doi:10.1021/Es60138a014.

Skamarock, W. C., et al. (2008), A description of the advanced research WRF version 3. NCAR Tech. Note TN-475_STR, 113 pp.

Smedman, A. S., M. Tjernstrom, and U. Hogstrom (1993), Analysis of the turbulence structure of a marine low-level jet, *Bound-Lay Meteorol.*, *66*(1–2), 105–126, doi:10.1007/Bf00705462.

Smedman, A. S., H. Bergstrom, and U. Hogstrom (1995), Spectra, variances and length scales in a marine stable boundary layer dominated by a low level jet, *Bound-Lay Meteorol.*, *76*(3), 211–232, doi:10.1007/Bf00709352.

Srinivas, C. V., R. Venkatesan, and A. B. Singh (2007), Sensitivity of mesoscale simulations of land-sea breeze to boundary layer turbulence parameterization, *Atmos. Environ.*, *41*(12), 2534–2548, doi:10.1016/j.atmosenv.2006.11.027.

Steeneveld, G. J., B. J. H. Van de Wiel, and A. A. M. Holtslag (2006), Modelling the Arctic Stable boundary layer and its coupling to the surface, *Bound-Lay Meteorol.*, *118*(2), 357–378, doi:10.1007/s10546-005-7771-z.

Steeneveld, G. J., T. Mauritsen, E. I. F. de Bruijn, J. V. G. de Arellano, G. Svensson, and A. A. M. Holtslag (2008), Evaluation of limited-area models for the representation of the diurnal cycle and contrasting nights in CASES-99, *J. Appl. Meteorol. Climatol.*, *47*(3), 869–887, doi:10.1175/2007jamc1702.1.

Sterk, H. A. M., G. J. Steeneveld, and A. A. M. Holtslag (2013), The role of snow-surface coupling, radiation, and turbulent mixing in modeling a stable boundary layer over Arctic sea ice, *J Geophys Res. Atmos*, *118*, 1199–1217, doi:10.1002/jgrd.50158.

Stockwell, W. R., F. Kirchner, M. Kuhn, and S. Seefeld (1997), A new mechanism for regional atmospheric chemistry modeling, *J. Geophys. Res.*, *102*(D22), 25,847–25,879, doi:10.1029/97JD00849.

Stockwell, W., R. Fitzgerald, D. Lu, and R. Perea (2013), Differences in the variability of measured and simulated tropospheric ozone mixing ratios over the Paso del Norte Region, *J. Atmos. Chem.*, *70*(1), 91–104, doi:10.1007/s10874-013-9253-x.

Storm, B., and S. Basu (2010), The WRF model forecast-derived low-level wind shear climatology over the United States Great Plains, *Energies*, *3*(2), 258–276, doi:10.3390/En3020258.

Storm, B., J. Dudhia, S. Basu, A. Swift, and I. Giammanco (2009), Evaluation of the weather research and forecasting model on forecasting low-level jets: Implications for wind energy, *Wind Energy*, *12*(1), 81–90, doi:10.1002/We.288.

Stutz, J., B. Alicke, R. Ackermann, A. Geyer, A. White, and E. Williams (2004), Vertical profiles of NO_3, N_2O_5, O_3, and NO_x in the nocturnal boundary layer: 1. Observations during the Texas Air Quality Study 2000, *J. Geophys. Res.*, *109*, D12306, doi:10.1029/2003JD004209.

Svensson, G., et al. (2011), Evaluation of the diurnal cycle in the atmospheric boundary layer over land as represented by a variety of single-column models: The second GABLS experiment, *Bound-Lay Meteorol*, *140*(2), 177–206, doi:10.1007/s10546-011-9611-7.

Teixeira, J., et al. (2008), Parameterization of the atmospheric boundary layer, *Bull. Am. Meteorol. Soc.*, *89*(4), 453–458, doi:10.1175/Bams-89-4-453.

Todd, M. C., R. Washington, S. Raghavan, G. Lizcano, and P. Knippertz (2008), Regional model simulations of the Bodele low-level jet of northern Chad during the Bodele Dust Experiment (BoDEx 2005), *J. Clim.*, *21*(5), 995–1012, doi:10.1175/2007jcli1766.1.

Van de Wiel, B. J. H., R. J. Ronda, A. F. Moene, H. A. R. De Bruin, and A. A. M. Holtslag (2002), Intermittent turbulence and oscillations in the stable boundary layer over land, Part I: A bulk model, *J. Atmos. Sci.*, *59*(5), 942–958, doi:10.1175/1520-0469(2002)059<0942:Itaoit>2.0.Co;2.

Vautard, R., et al. (2012), Evaluation of the meteorological forcing used for the Air Quality Model Evaluation International Initiative (AQMEII) air quality simulations, *Atmos. Environ.*, *53*, 15–37, doi:10.1016/j.atmosenv.2011.10.065.

Viterbo, P., A. Beljaars, J. F. Mahfouf, and J. Teixeira (1999), The representation of soil moisture freezing and its impact on the stable boundary layer, *Q. J. Roy Meteor. Soc.*, *125*(559), 2401–2426, doi:1256/Smsqj.55903.

Wexler, H. (1961), A boundary layer interpretation of the low-level jet, *Tellus*, *13*(3), 368–378.

Wolff, J., and M. Harrold (2013), Tracking WRF performance: How do the three most recent versions compare? The 14th annual WRF users' workshop, paper 2.6, http://www.mmm.ucar.edu/wrf/users/workshops/WS2013/ppts/2.6.pdf.

Xie, B., J. C. H. Fung, A. Chan, and A. Lau (2012), Evaluation of nonlocal and local planetary boundary layer schemes in the WRF model, *J. Geophys. Res.*, *117*, D12103, doi:10.1029/2011JD017080.

Xie, B., J. C. R. Hunt, D. J. Carruthers, J. C. H. Fung, and J. F. Barlow (2013), Structure of the planetary boundary layer over Southeast England: Modeling and measurements, *J. Geophys. Res. Atmos.*, *118*, 7799–7818, doi:10.1002/jgrd.50621.

Yang, Q., L. K. Berg, M. Pekour, J. D. Fast, R. K. Newsom, M. Stoelinga, and C. Finley (2013), Evaluation of WRF-predicted near-hub-height winds and ramp events over a Pacific Northwest site with complex terrain, *J. Appl. Meteorol. Climatol.*, *52*(8), 1753–1763, doi:10.1175/Jamc-D-12-0267.1.

Yu, S. C., B. Eder, R. Dennis, S. H. Chu, and S. E. Schwartz (2006), New unbiased symmetric metrics for evaluation of air quality models, *Atmos Sci Lett*, *7*(1), 26–34, doi:10.1002/Asl.125.

Yver, C. E., H. D. Graven, D. D. Lucas, P. J. Cameron-Smith, R. F. Keeling, and R. F. Weiss (2013), Evaluating transport in the WRF model along the California coast, *Atmos. Chem. Phys.*, *13*(4), 1837–1852, doi:10.5194/acp-13-1837-2013.

Žabkar, R., J. Rakovec, and D. Koracin (2011), The roles of regional accumulation and advection of ozone during high ozone episodes in Slovenia: A WRF/Chem modelling study, *Atmos. Environ.*, *45*(5), 1192–1202, doi:10.1016/j.atmosenv.2010.08.021.

Žabkar, R., D. Koračin, and J. Rakovec (2013), A WRF/Chem sensitivity study using ensemble modelling for a high ozone episode in Slovenia and the Northern Adriatic area, *Atmos. Environ.*, *77*(0), 990–1004, doi:10.1016/j.atmosenv.2013.05.065.

Zhang, D. L., and W. Z. Zheng (2004), Diurnal cycles of surface winds and temperatures as simulated by five boundary layer parameterizations, *J. Appl. Meteorol.*, *43*(1), 157–169, doi:10.1175/1520-0450(2004)043<0157:Dcoswa>2.0.Co;2.

Zhang, Y., M. K. Dubey, S. C. Olsen, J. Zheng, and R. Zhang (2009), Comparisons of WRF/Chem simulations in Mexico City with ground-based RAMA measurements during the 2006-MILAGRO, *Atmos. Chem. Phys.*, *9*(11), 3777–3798, doi:10.5194/acp-9-3777-2009.

Zhang, H., Z. Pu, and X. Zhang (2013), Examination of errors in near-surface temperature and wind from WRF numerical simulations in regions of complex terrain, *Weather Forecast*, *28*(3), 893–914, doi:10.1175/Waf-D-12-00109.1.

Zilitinkevich, S. S., T. Elperin, N. Kleeorin, and I. Rogachevskii (2007), Energy- and flux-budget (EFB) turbulence closure model for stably stratified flows. Part I: Steady-state, homogeneous regimes, *Bound-Lay Meteorol.*, *125*(2), 167–191, doi:10.1007/s10546-007-9189-2.